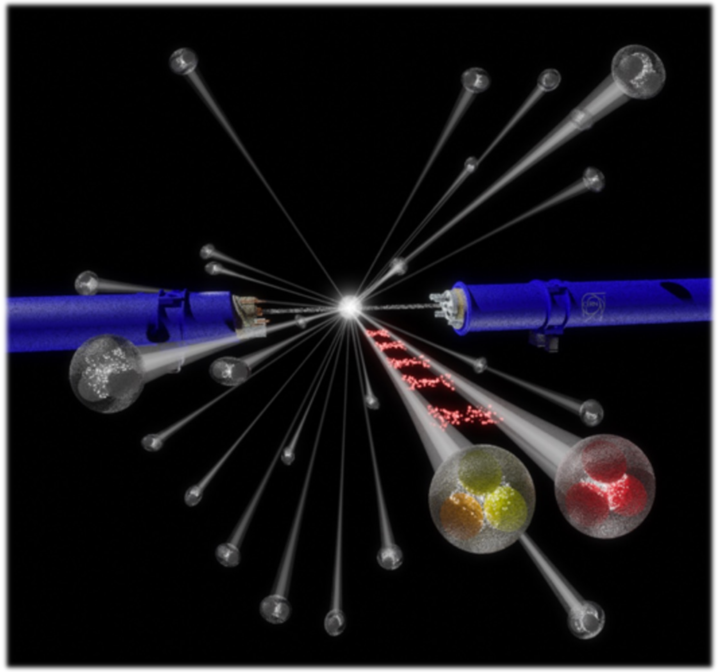

Accessing the coupled-channels dynamics using femtoscopic correlations with ALICE at LHC

V. Mantovani Sarti (TUM) on behalf of the ALICE Collaboration

Baryons 2022 – 07.11.2022

Motivation: inelastic channels in h-h interactions

- Coupled-channel dynamics widely present in hadron-hadron strong interactions
  - Close in mass and same quantum numbers (e.g. B,S,Q)
  - On-shell and off-shell processes from one channel to the other
- Can be at the origin of several phenomena
  - Molecular states as Λ(1405) → interplay of $\bar{K}N$–Σπ
- Annihilation dynamics for B–$\bar{B}$ interactions
  - Multi-meson channels below threshold

Talk by Dr. Y. Kamiya
07.11 17:00

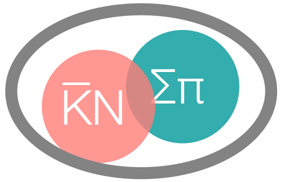

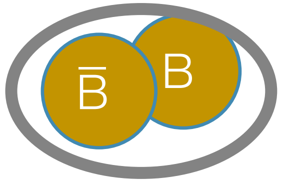

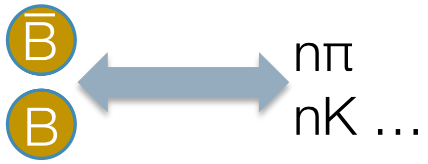

Prog.Part.Nucl.Phys. 67 (2012) 55-98

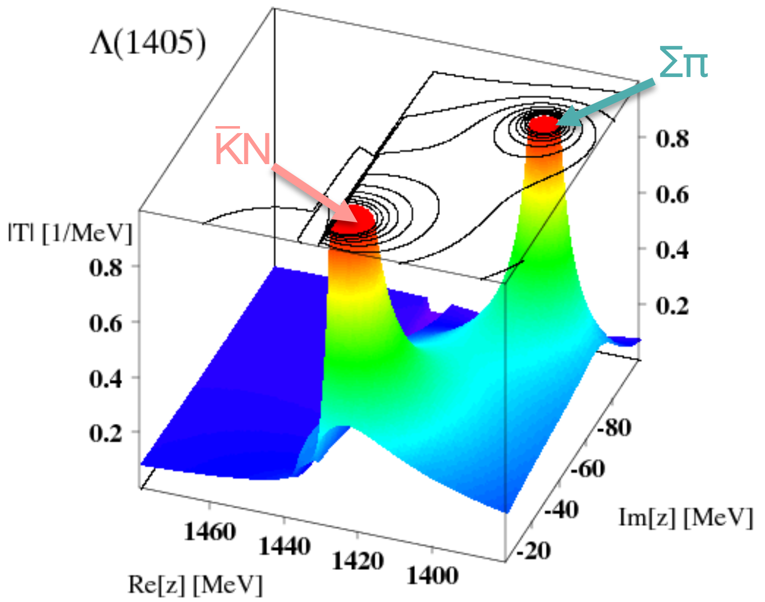

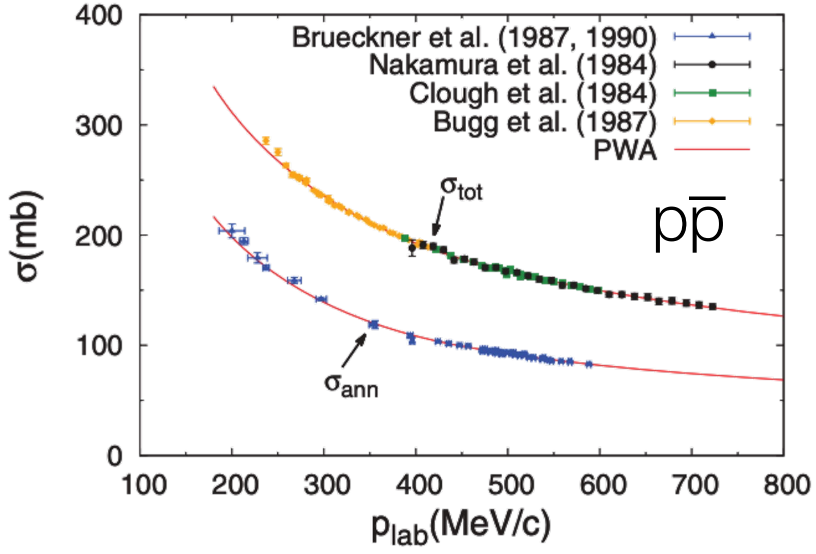

D. Zhou and R.G. E. Timmermans PRC86 (2012)

Femtoscopy in ALICE with inelastic channels

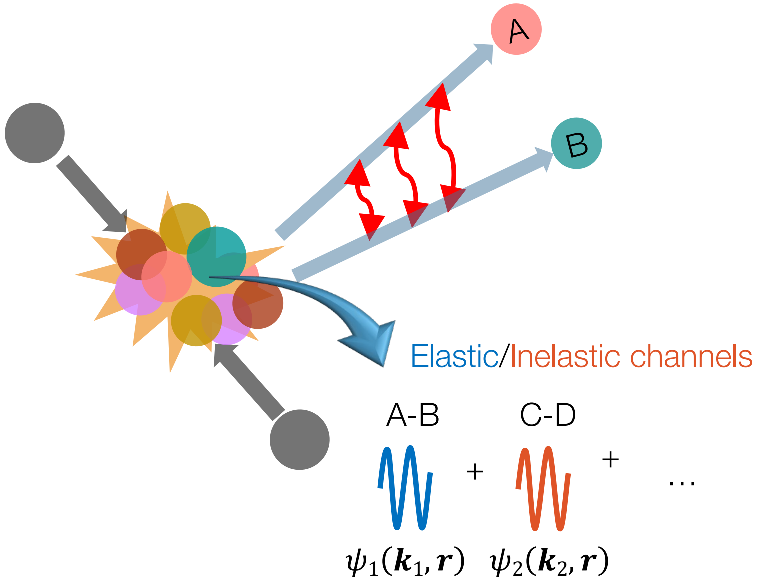

$$C_{A-B}(k^*) = \int S(r)\ |\psi_{1\to 1}(k^*, r)|^2\, d^3r + \sum_{j\neq 1} \omega_j^{prod} \int S(r)\ \left|\psi_{j\to 1}(k_j^*, r)\right|^2 d^3r = \mathcal{N}(k^*)\frac{N_{same}(k^*)}{N_{mixed}(k^*)}$$

elastic
A-B → A-B

inelastic
C-D → A-B, …

Femtoscopy in ALICE with inelastic channels

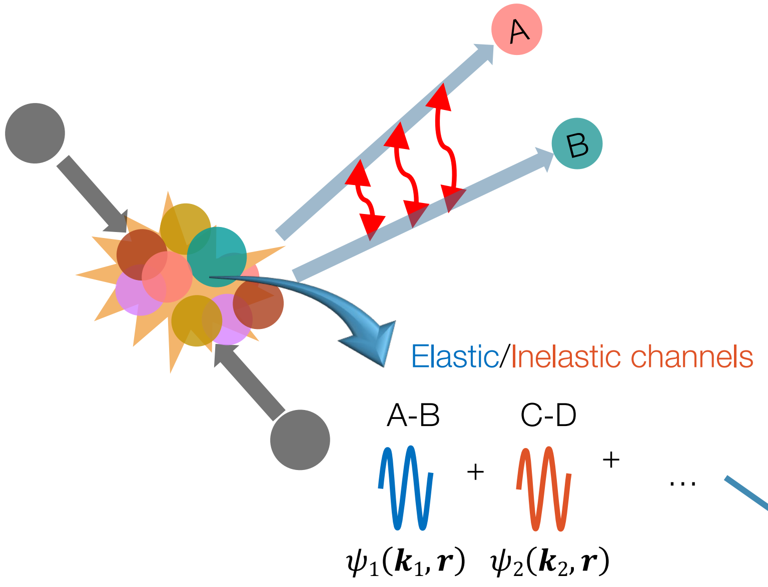

- Conversion weights ω_j
  - inelastic channels produced pairs as initial states
    - depends on yields and kinematics
    - thermal models and transport/blast wave models

$$C_{A-B}(k^*) = \int S(r)\ |\psi_{1\to1}(k^*, r)|^2\, d^3r + \sum_{j\neq1} \omega_j^{prod} \int S(r)\ |\psi_{j\to1}(k_j^*, r)|^2\, d^3r = \mathcal{N}(k^*)\frac{N_{same}(k^*)}{N_{mixed}(k^*)}$$

elastic
A-B → A-B

inelastic
C-D → A-B, …

V. Vovchenko et al., PRC 100 no. 5 (2019))
E. Schnedermann et al., PRC 48 (1993)
ALICE Coll., PLB 728 (2014)
ALICE Coll., PRC 101 no. 4 (2020)

Femtoscopy in ALICE with inelastic channels

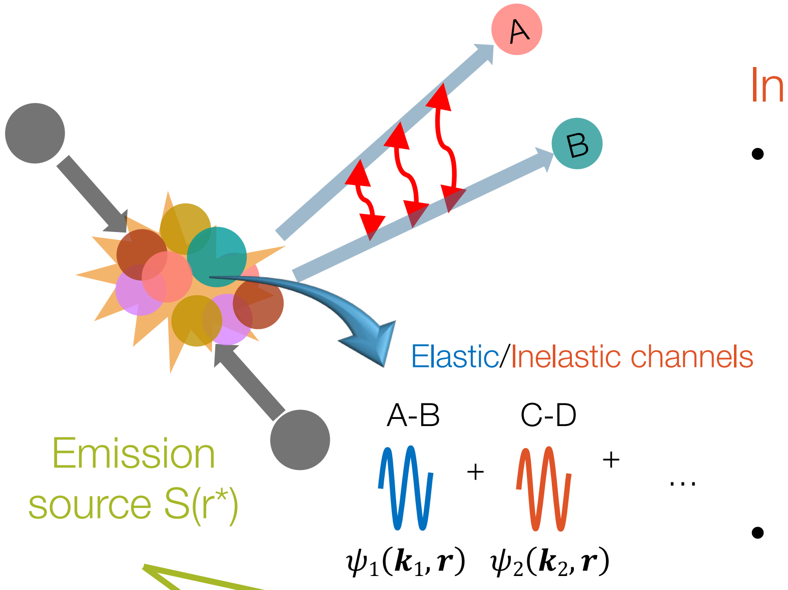

In small colliding systems:

- Gaussian r_{core} + resonance source model
  - anchored to known interactions (pp, K^+p)
  - universal emitting source for particles
- Effective Gaussian with r_G ~1-2 fm

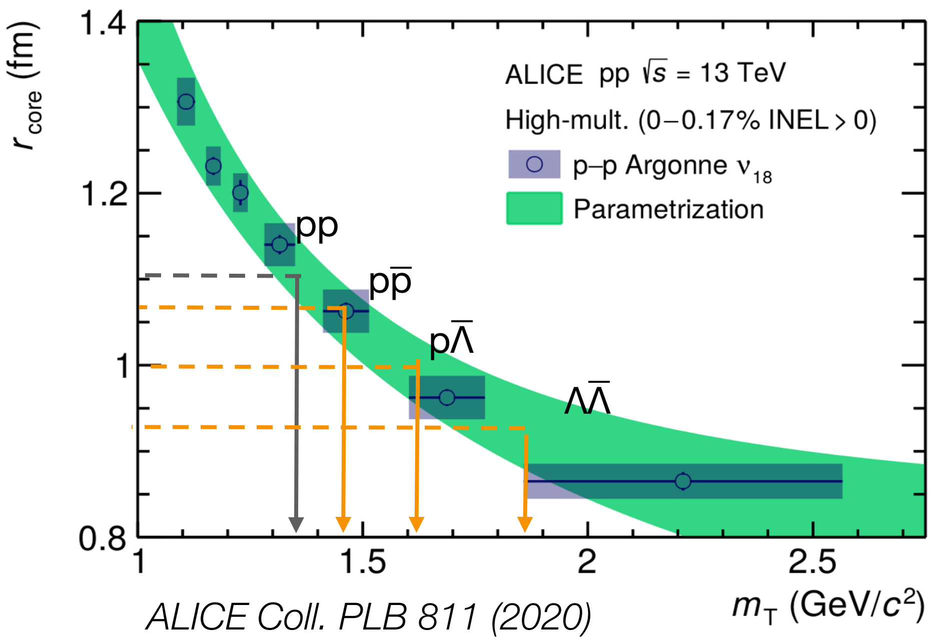

ALICE Coll. PLB 811 (2020)

$$C_{A-B}(k^*) = \int S(r)\, |\psi_{1\to1}(k^*, r)|^2\, d^3r + \sum_{j\neq1} \omega_j^{prod} \int S(r)\, \left|\psi_{j\to1}(k_j^*, r)\right|^2 d^3r = \mathcal{N}(k^*)\,\frac{N_{same}(k^*)}{N_{mixed}(k^*)}$$

elastic
A-B → A-B

inelastic
C-D → A-B, …

Femtoscopy in ALICE with inelastic channels

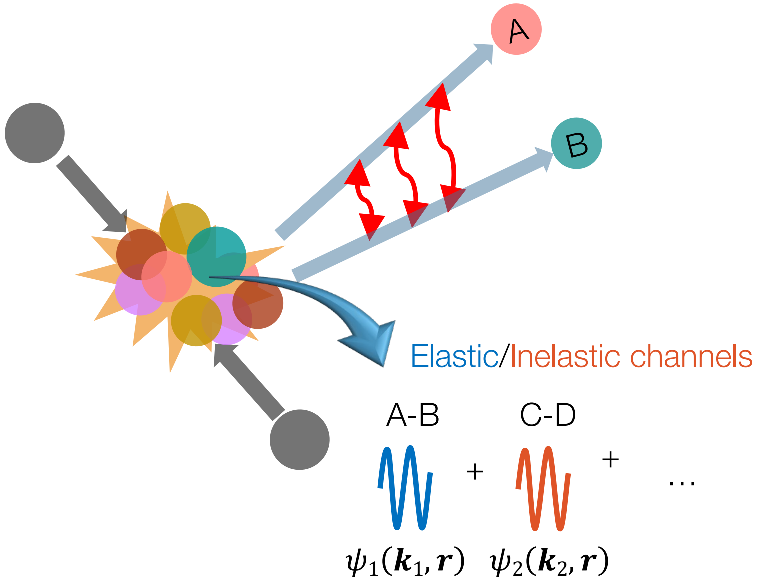

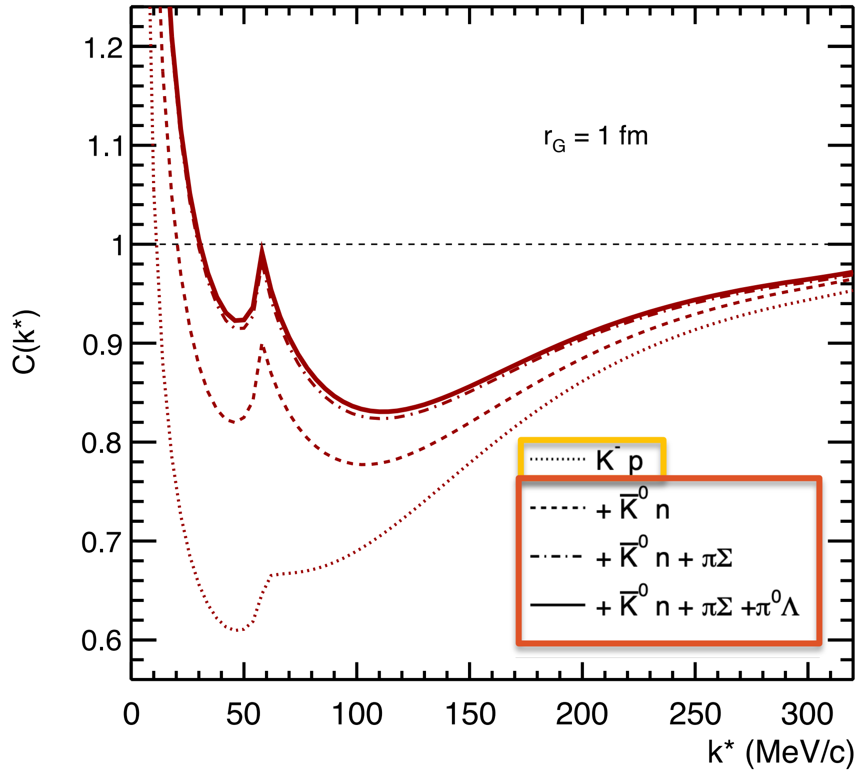

1. Above threshold: modify the shape of CF → cusp structure e.g. $\bar{K}^0 n$
2. Below threshold: increase the strength of CF → shift upward of CF e.g. $\Sigma\pi$

$$C_{A-B}(k^*) = \int S(r)\, |\psi_{1\to 1}(k^*, r)|^2\, d^3r + \sum_{j\neq 1} \omega_j^{prod} \int S(r)\, |\psi_{j\to 1}(k_j^*, r)|^2\, d^3r = \mathcal{N}(k^*) \frac{N_{same}(k^*)}{N_{mixed}(k^*)}$$

elastic
A-B → A-B

inelastic
C-D → A-B, …

CATS: D. Mihaylov, VMS et al. EPJC 78 (2019)
J. Haidenbauer Nucl.Phys.A 981 (2019)
Y. Kamiya et al. Phys.Rev.Lett. 124 (2020)
VMS et al. Ann.Rev.Nucl.Part.Sci. 71 (2021)

Femtoscopy in ALICE with inelastic channels

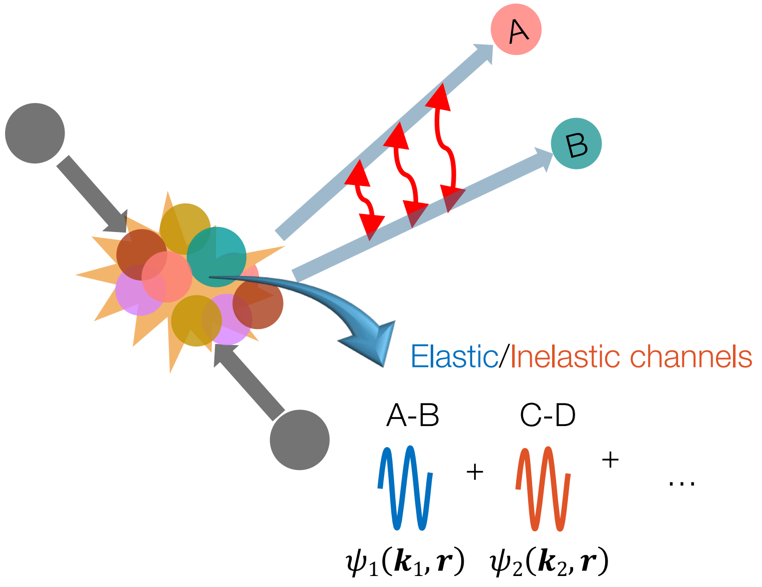

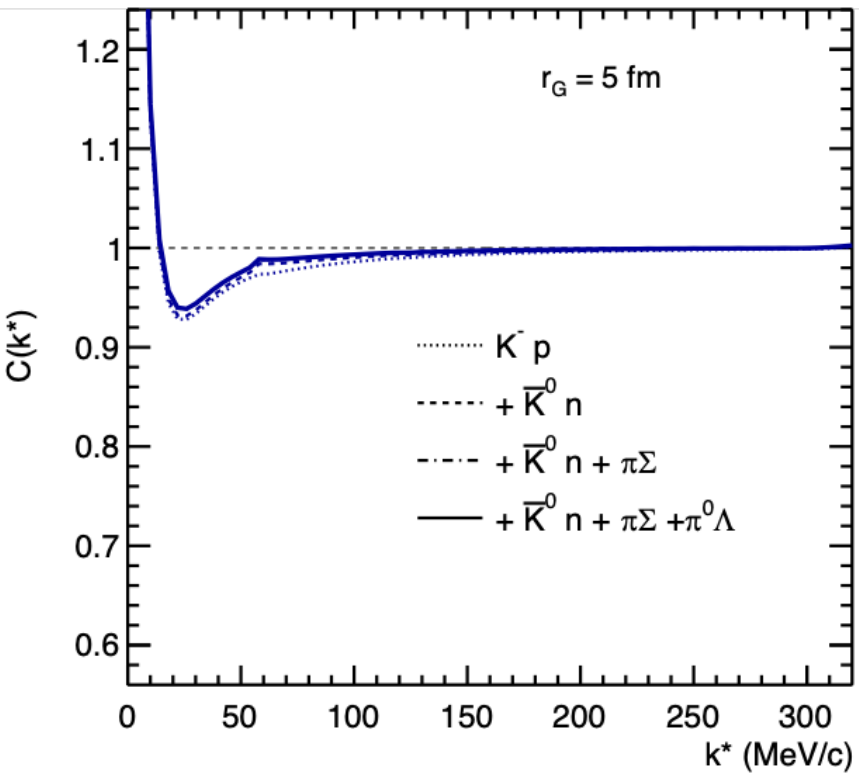

- Inelastic contributions effect on CF negligible as the source size increases
- For large source sizes → CF mainly driven by elastic interaction

$$C_{A-B}(k^*) = \int S(r)\,|\psi_{1\to1}(k^*,r)|^2\,d^3r + \sum_{j\neq1} \omega_j^{prod} \int S(r)\,\left|\psi_{j\to1}(k_j^*,r)\right|^2 d^3r = \mathcal{N}(k^*)\frac{N_{same}(k^*)}{N_{mixed}(k^*)}$$

elastic
A-B → A-B

inelastic
C-D → A-B, …

CATS: D. Mihaylov, VMS et al. EPJC 78 (2019)
J. Haidenbauer Nucl.Phys.A 981 (2019)
Y. Kamiya et al. Phys.Rev.Lett. 124 (2020)
VMS et al. Ann.Rev.Nucl.Part.Sci. 71 (2021)

Inelastic channels and source size dependence

- Scan of measured correlation for different source sizes
  - K^--p (K^+-p) in pp 13 TeV, p–Pb 0-100% and Pb–Pb 70–90% 5.02 TeV
  - p-$\overline{\Lambda}$ and Λ-$\overline{\Lambda}$ in pp HM 13 TeV and Pb–Pb 5.02 TeV

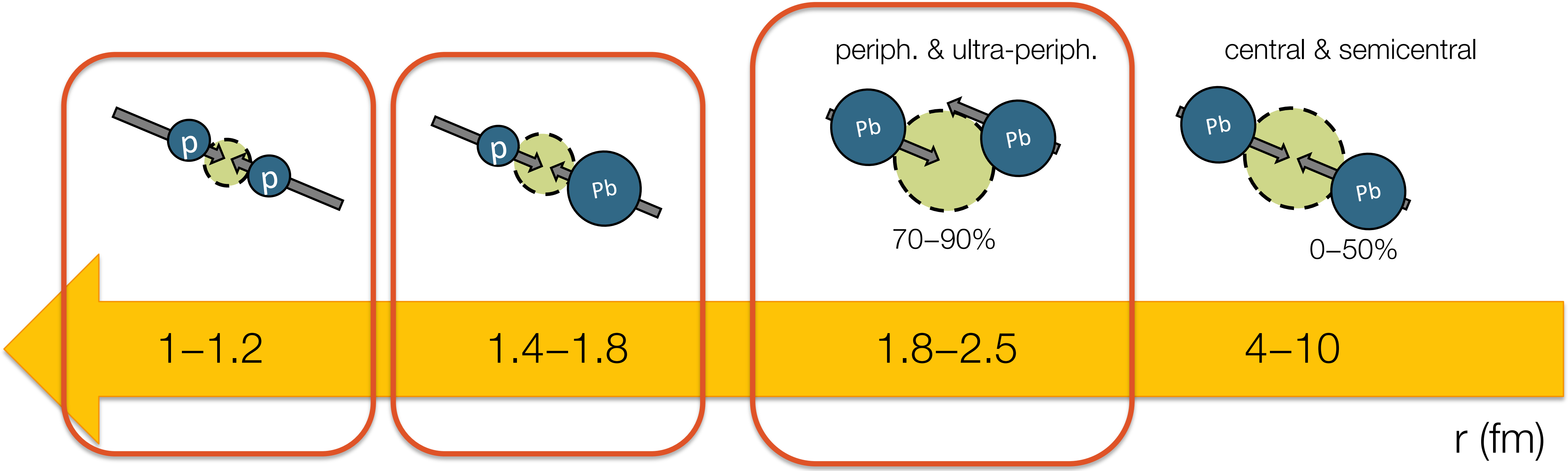

K^--p and K^+-p femtoscopy

K⁻-p femtoscopy: the antiKaon-nucleon interaction

Λ(1405) molecular state

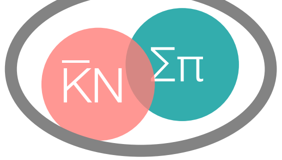

A. Cieplý et al., arxiv:2001.08621

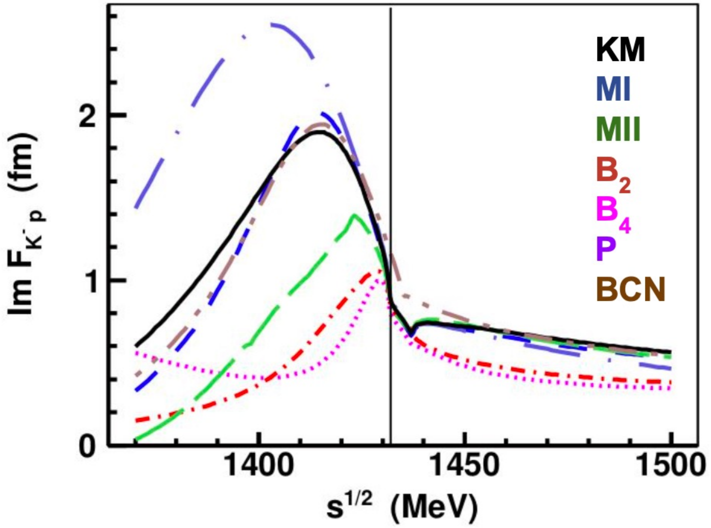

Kaonic hydrogen

SIDDHARTA Coll. PLB 704 (2011)

Scattering Experiments

Ikeda et al. Nucl.Phys.A 881 (2012)

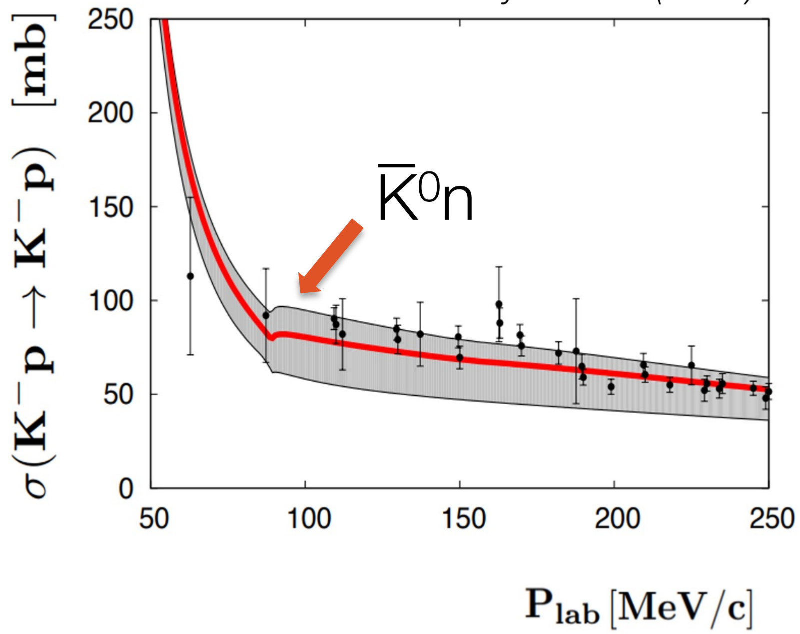

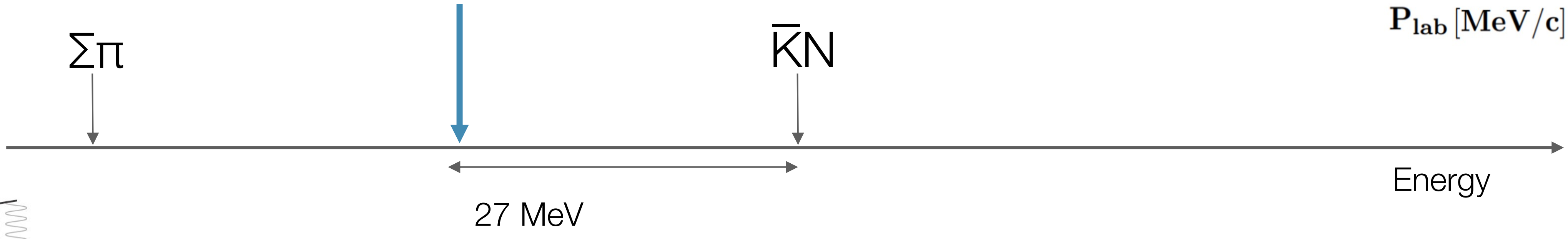

K⁻-p femtoscopy: the antiKaon-nucleon interaction

Λ(1405) molecular state

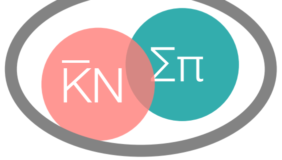

A. Cieplý et al., arxiv:2001.08621

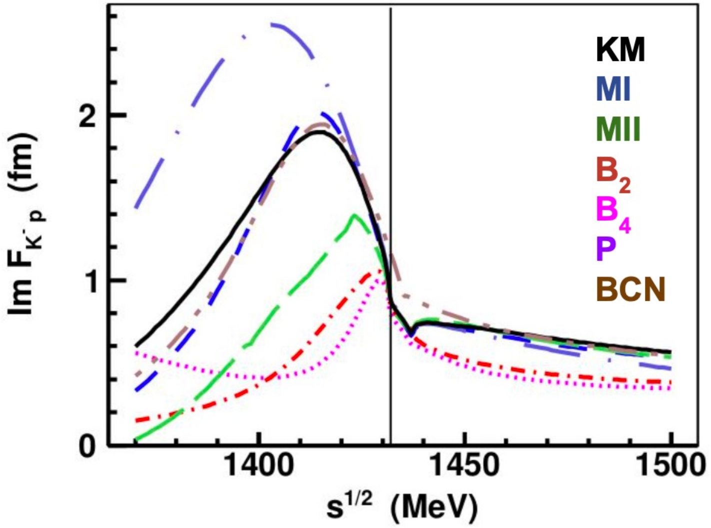

Kaonic hydrogen

SIDDHARTA Coll. PLB 704 (2011)

Femtoscopy with ALICE

Scattering Experiments

Ikeda et al. Nucl.Phys.A 881 (2012)

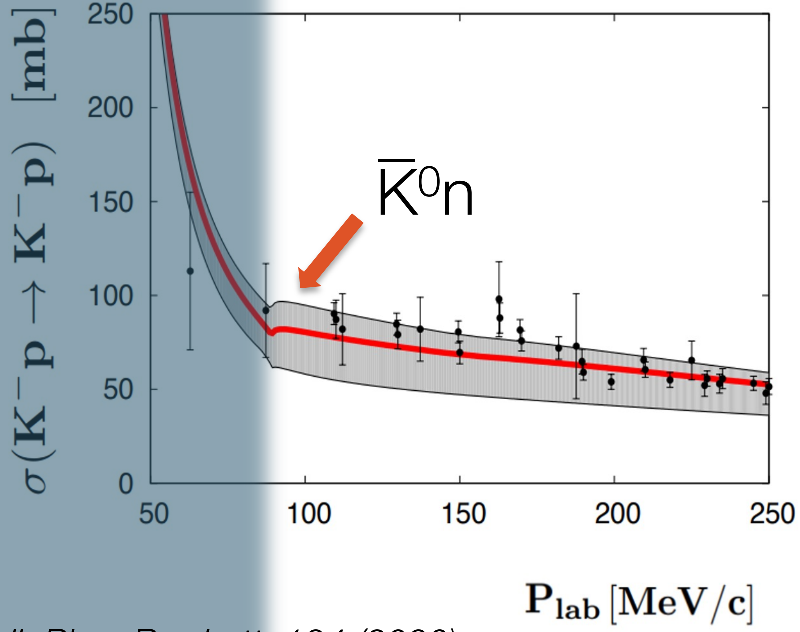

ALICE Coll. Phys.Rev.Lett. 124 (2020)

ALICE Coll. Phys.Lett.B 822 (2021)

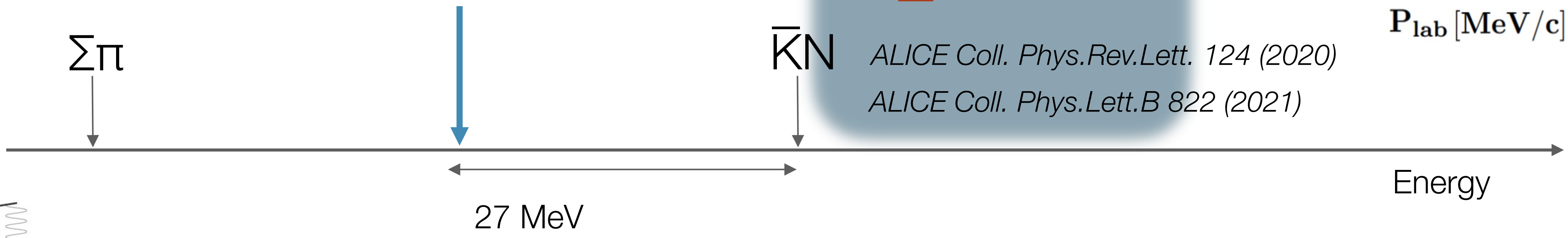

K^-–p femtoscopy in different colliding systems

Talk by Prof.T.Hyodo
07.11 15:00

ALICE

Fixed conversion weights: statistical model + Blast wave fit

$$C(k^*) = \int S(r)\, \left|\psi_{1\to1}(k^*, r)\right|^2 d^3r + \sum_{j=\Sigma\pi,\bar{K}^0n} \omega_j^{prod} \int S_j(r)\, \left|\psi_{j\to1}(k_j^*, r)\right|^2 d^3r$$

χEFT Kyoto model:
Ikeda et al. NPA 881 (2012), PLB706 (2011)
Kamiya et al. PRL 124 (2020)
Mihayara et al. PRC95 (2017)

Data: ALICE Coll. Phys.Rev.Lett. 124 (2020)

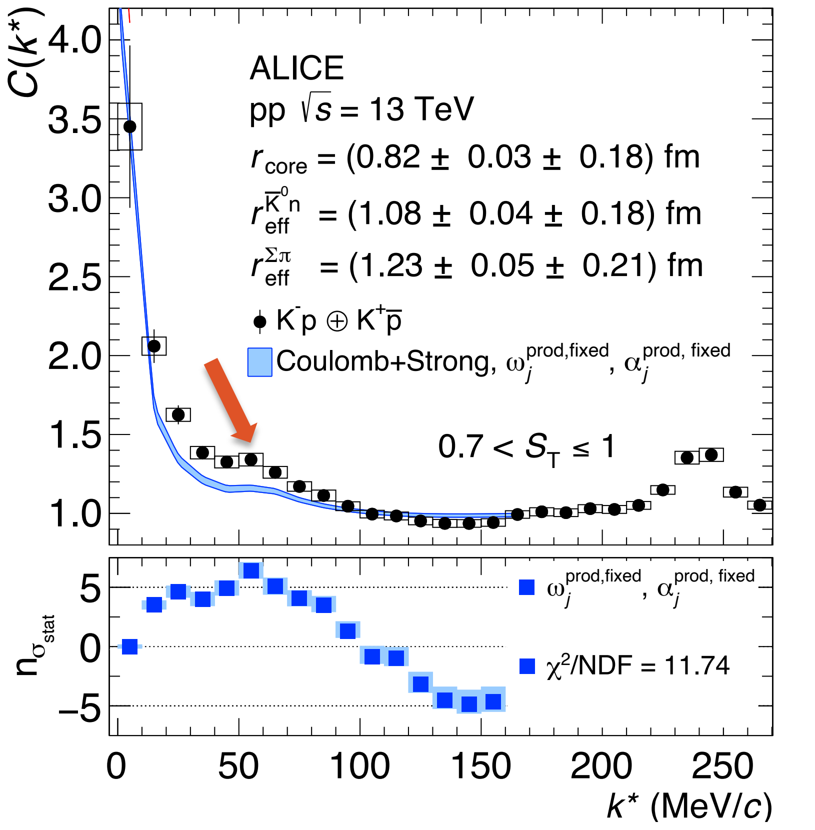

ALICE Coll. arXiv:2205.15176, accepted by EPJC

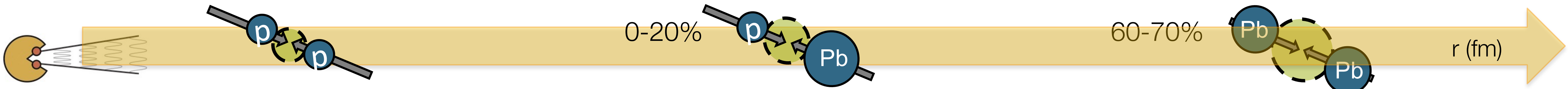

K^-–p femtoscopy in different colliding systems

Talk by Prof.T.Hyodo
07.11 15:00

ALICE

Fixed conversion weights: statistical model + Blast wave fit

$$C(k^*) = \int S(r) \left|\psi_{1\to1}(k^*, r)\right|^2 d^3r + \sum_{j=\Sigma\pi,\bar{K}^0 n} \omega_j^{prod} \int S_j(r) \left|\psi_{j\to1}(k_j^*, r)\right|^2 d^3r$$

χEFT Kyoto model:
Ikeda et al. NPA 881 (2012), PLB706 (2011)
Kamiya et al. PRL 124 (2020)
Mihayara et al. PRC95 (2017)

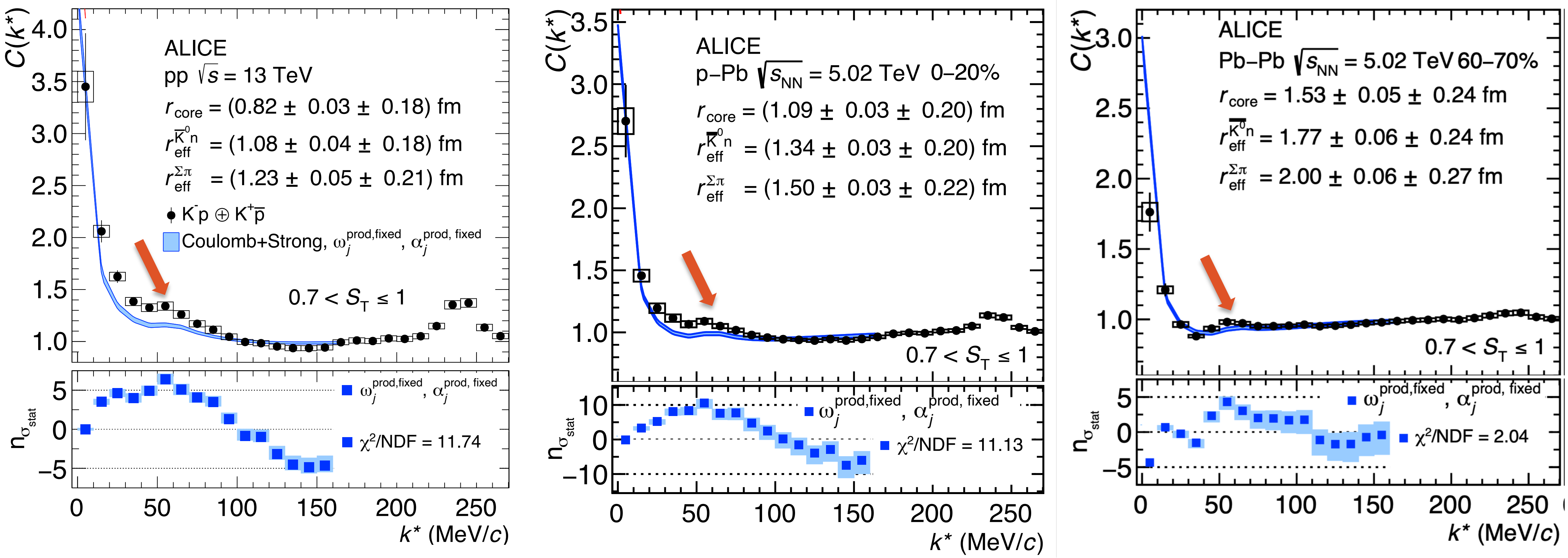

ALICE Coll. arXiv:2205.15176, accepted by EPJC

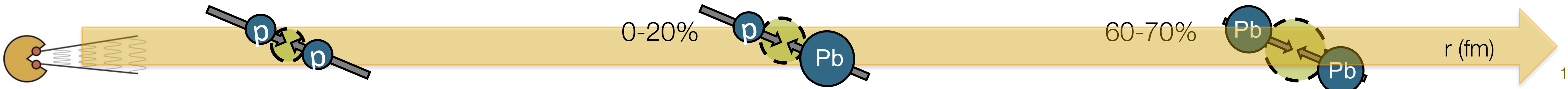

K⁻–p femtoscopy in different colliding systems

Talk by Prof.T.Hyodo
07.11 15:00

Fit the scaling factor needed for the model to reproduce the data

$$C(k^*) = \int S(r)\,\left|\psi_{1\to1}(k^*,r)\right|^2 d^3r + \sum_{j=\Sigma\pi,\bar{K}^0n} \alpha_j \cdot \omega_j^{prod} \int S_j(r)\,\left|\psi_{j\to1}(k_j^*,r)\right|^2 d^3r$$

χEFT Kyoto model:
Ikeda et al. NPA 881 (2012), PLB706 (2011)
Kamiya et al. PRL 124 (2020)
Mihayara et al. PRC95 (2017)

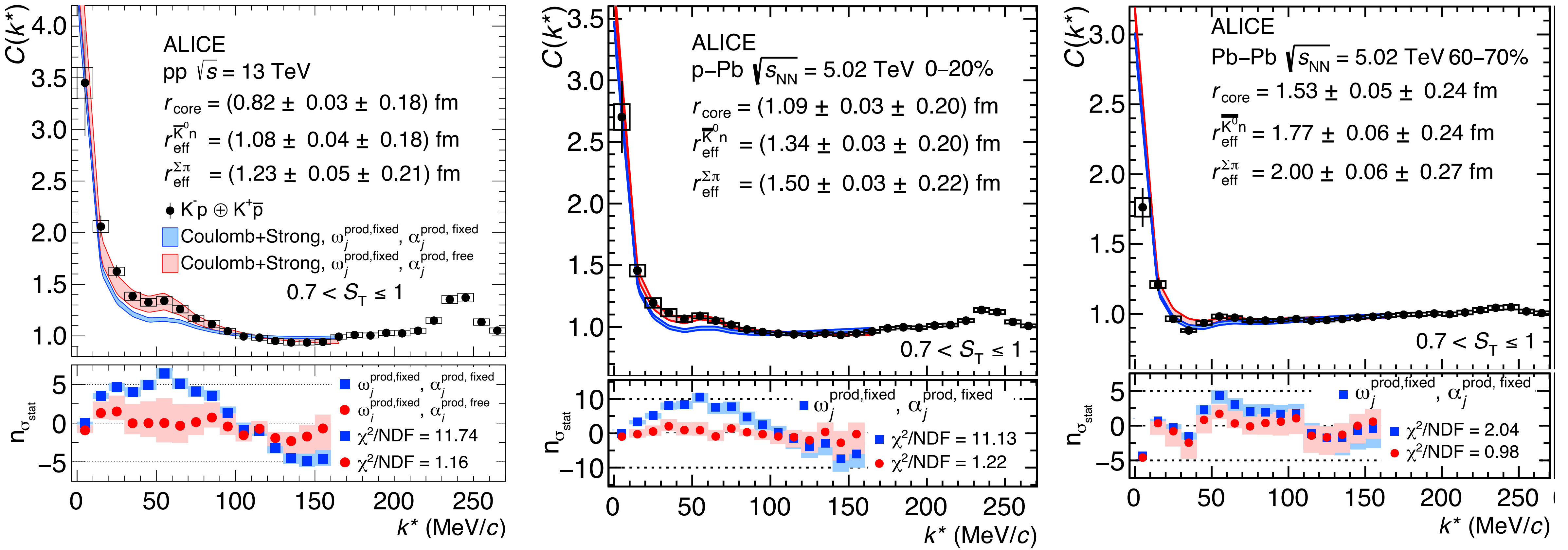

ALICE Coll. arXiv:2205.15176, accepted by EPJC

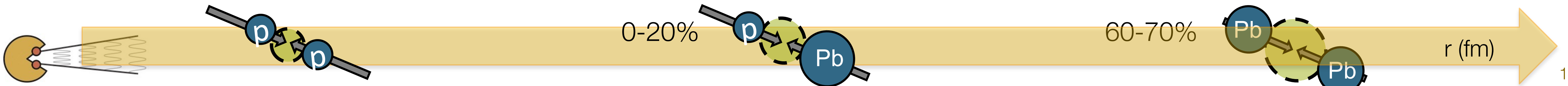

Extracted strong weights for Σπ and $\overline{K}^0$ n channels

Unique constraint and direct access to $K^-p \leftrightarrow \overline{K}^0 n$ and $K^-p \leftrightarrow \Sigma\pi$ dynamics

- Σπ consistent with unity
- deviation from unity for $\overline{K}^0$ n
  - K^-p - $\overline{K}^0$ n coupling too weak in chiral potentials
  - update the scattering amplitude of KN–πΣ–πΛ system by including correlation measurements to available kaonic hydrogen and scattering data

ALICE Coll. arXiv:2205.15176, accepted by EPJC

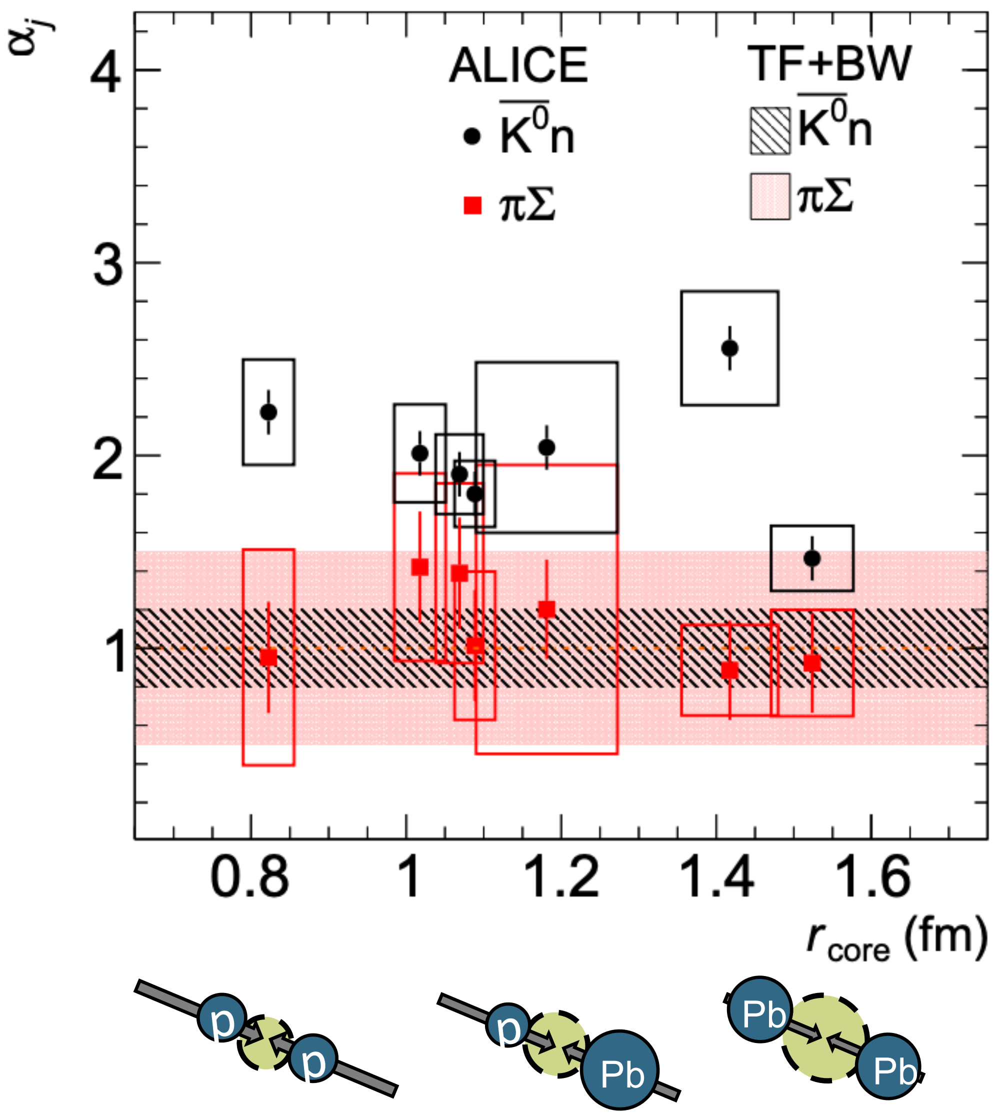

Baryon-antibaryon femtoscopy

The baryon-antibaryon interaction with strangeness

ALICE

Predictions for Baryonia??

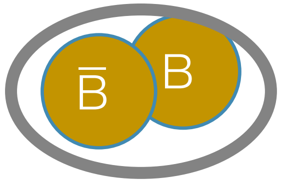

?

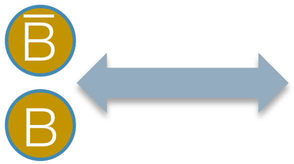

nπ
nK …

Annihilation dynamics
nπ,nK,πK,…

Protonium

Scattering Experiments

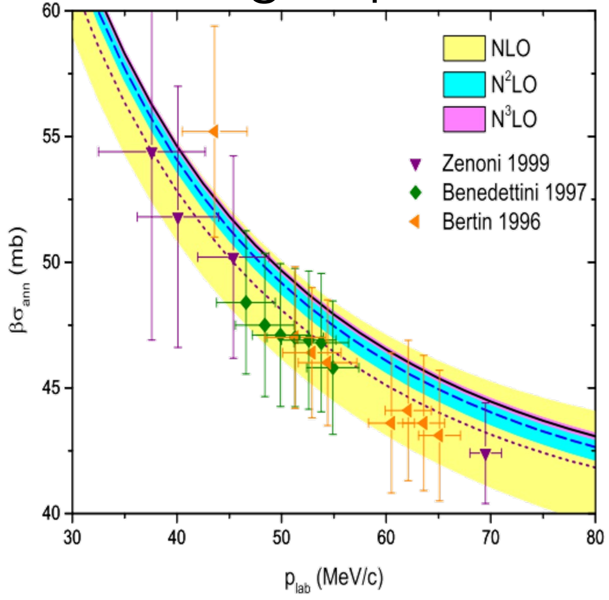

p-$\bar{p}$ p-$\bar{\Lambda}$ Λ-$\bar{\Lambda}$

177 MeV

Energy

E. Klempt et al. Phys. Rept. 413 (2005)
E. Klempt et al. Phys. Rept. 368 (2002)
D. Zhou and R.G. E. Timmermans PRC86 (2012)
J. Haidenbauer et al. JHEP 1707 (2017)

The baryon-antibaryon interaction with strangeness

Predictions for Baryonia??

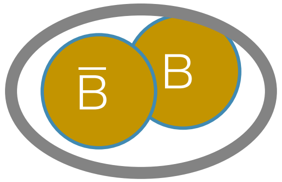

?

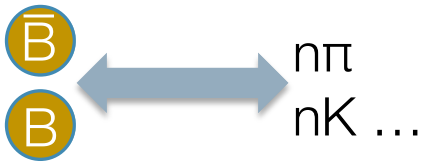

Annihilation dynamics
nπ,nK,πK,…

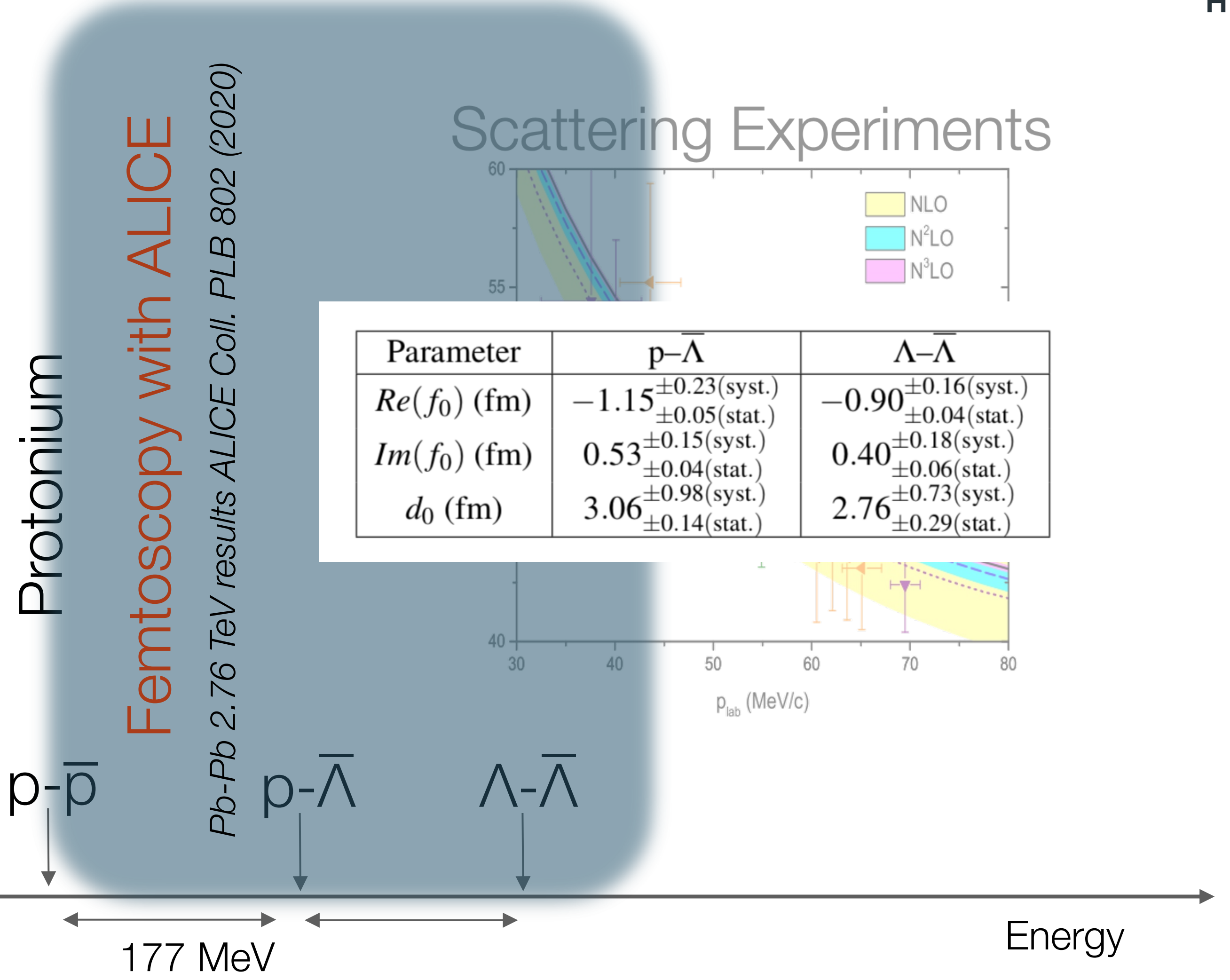

Parameter	p–Λ̄	Λ–Λ̄
$Re(f_0)$ (fm)	$-1.15^{\pm 0.23(\mathrm{syst.})}_{\pm 0.05(\mathrm{stat.})}$	$-0.90^{\pm 0.16(\mathrm{syst.})}_{\pm 0.04(\mathrm{stat.})}$
$Im(f_0)$ (fm)	$0.53^{\pm 0.15(\mathrm{syst.})}_{\pm 0.04(\mathrm{stat.})}$	$0.40^{\pm 0.18(\mathrm{syst.})}_{\pm 0.06(\mathrm{stat.})}$
d_0 (fm)	$3.06^{\pm 0.98(\mathrm{syst.})}_{\pm 0.14(\mathrm{stat.})}$	$2.76^{\pm 0.73(\mathrm{syst.})}_{\pm 0.29(\mathrm{stat.})}$

E. Klempt et al. Phys. Rept. 413 (2005)
E. Klempt et al. Phys. Rept. 368 (2002)
D. Zhou and R.G. E. Timmermans PRC86 (2012)
J. Haidenbauer et al. JHEP 1707 (2017)

Results on Λ-$\bar{\Lambda}$ and p-$\bar{\Lambda}$ femtoscopy

- No local potentials available → single-channel Lednický-Lyuboshits formula
- Assuming the scattering parameters obtained in Pb–Pb
  - nice agreement with Λ-$\bar{\Lambda}$ data → inelastic part present but not dominant

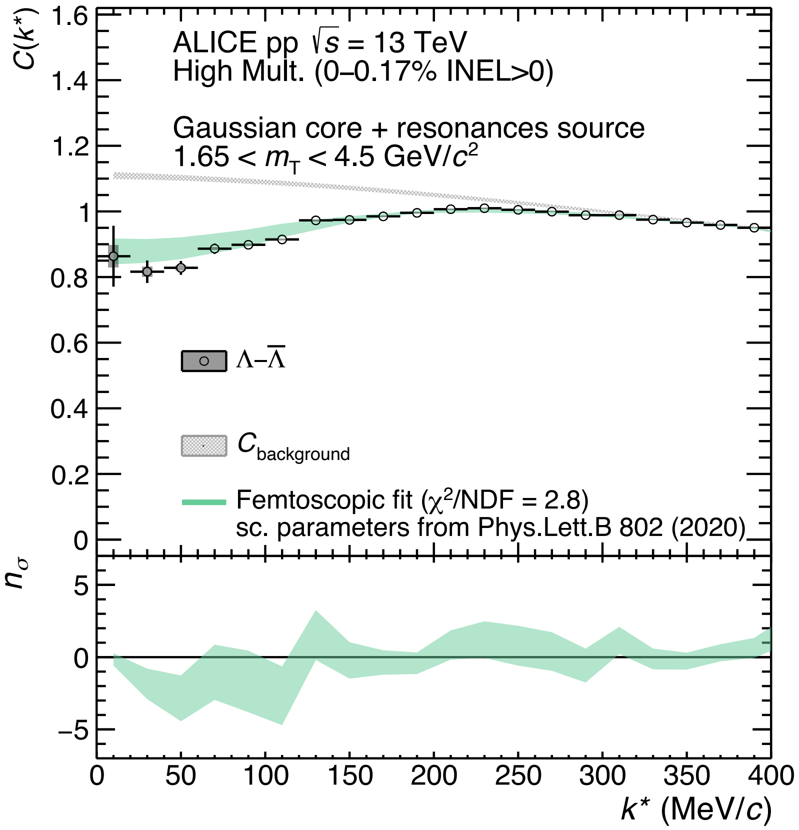

ALICE Coll. PLB 829 (2022)

Results on Λ-$\bar{\Lambda}$ and p-$\bar{\Lambda}$ femtoscopy

- No local potentials available → single-channel Lednický-Lyuboshits formula
- Assuming the scattering parameters obtained in Pb–Pb
  - nice agreement with Λ-$\bar{\Lambda}$ data → inelastic part present but not dominant
  - underestimate of p-$\bar{\Lambda}$ data → large coupling to multi-meson annihilation channels

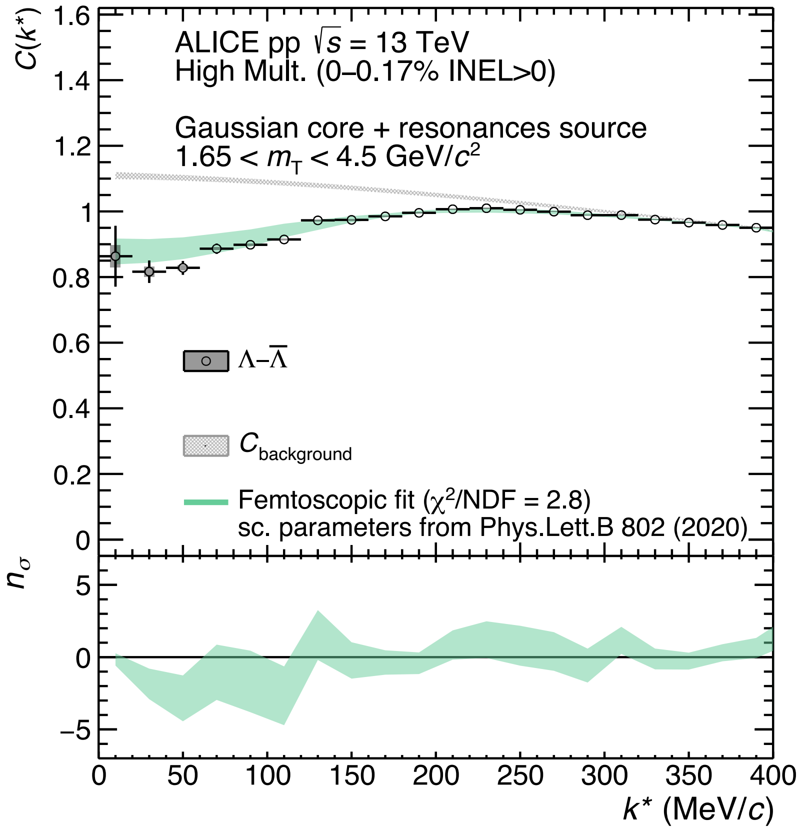

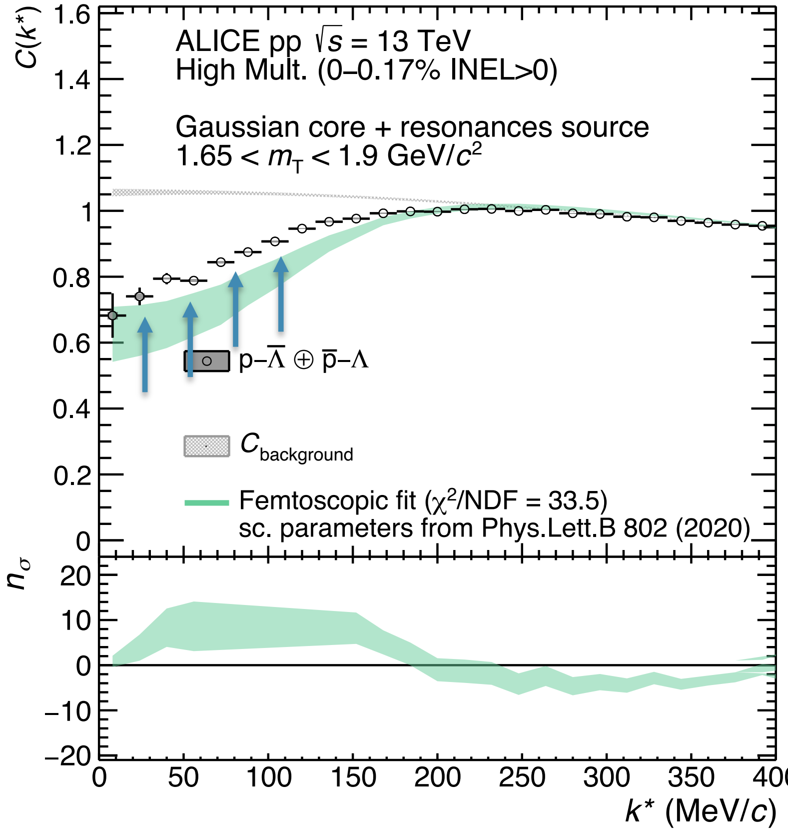

ALICE Coll. PLB 829 (2022)

Results on Λ-$\overline{\Lambda}$ and p-$\overline{\Lambda}$ femtoscopy

- Elastic part Re(f_0) fixed from Pb–Pb data, free inelastic Im(f_0) and d_0
  - extracted values for Λ-$\overline{\Lambda}$ are compatible with Pb–Pb scattering parameters
  - to reproduce p-$\overline{\Lambda}$ data Im(f_0) has to increased by a factor ~ 5.3
- Larger presence of multi-meson annihilation channels in p-$\overline{\Lambda}$ → no bound states?

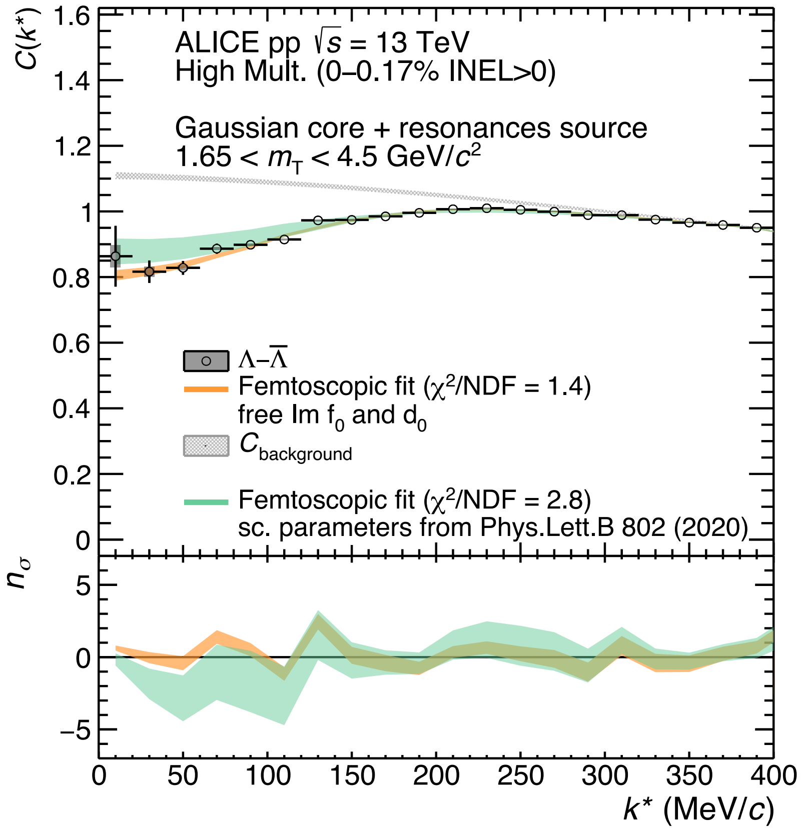

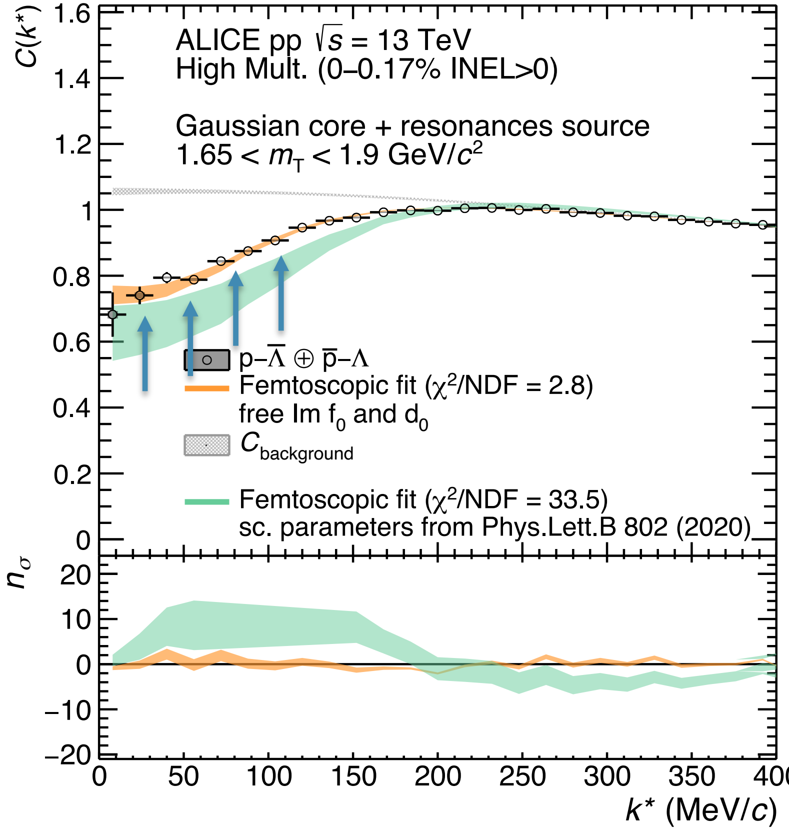

ALICE Coll. PLB 829 (2022)

Conclusions

- Femtoscopy in small and large colliding systems
  - high-precision data at low momenta
  - sensitivity to inelastic channels as a function of the source size
- K^-–p in pp, p–Pb and ultra-per. Pb–Pb collisions
  - first experimental evidence of $\bar{K}^0$ n opening
  - direct constraints on coupling to Σπ and $\bar{K}^0$ n
  - data suggests a stronger coupling to $\bar{K}^0$ n
- Baryon-antibaryon in pp collisions
  - Λ-$\bar{\Lambda}$ results annihilation not dominant and room for baryonia
  - p-$\bar{\Lambda}$ large presence of annihilation channels → no formation of bound states?
  - need for theoretical input on p-$\bar{\Lambda}$ and Λ-$\bar{\Lambda}$ interactions

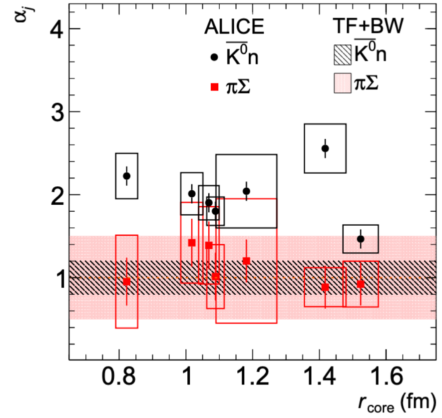

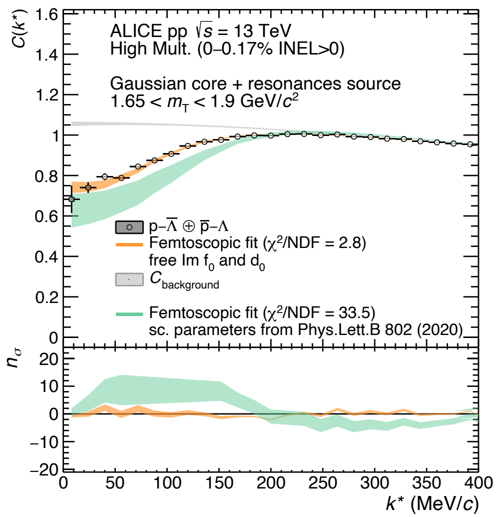

Additional slides

Scattering experiments…

- Fixed initial state (e.g.K^-) and different final states:
  - Elastic scattering: 1→1
  - Inelastic scattering: 1→2,3…

- Measurement of the cross section in different channels

- Disadvantages:
  - Not accessible down to zero momenta
  - Large uncertainties
  - Limited to few h-h interactions

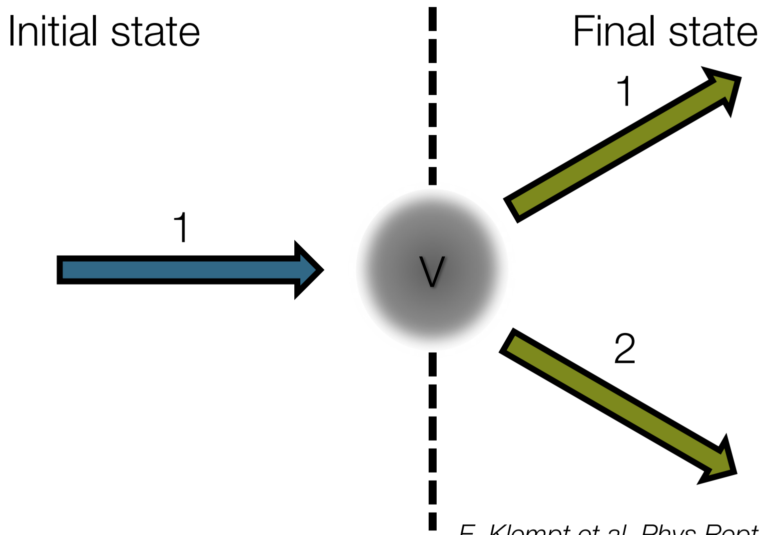

E. Klempt et al. Phys.Rept. 368 (2002) 119-316

G.S. Abrams et al. Phys.Rev. 139 (1965) B454-B457

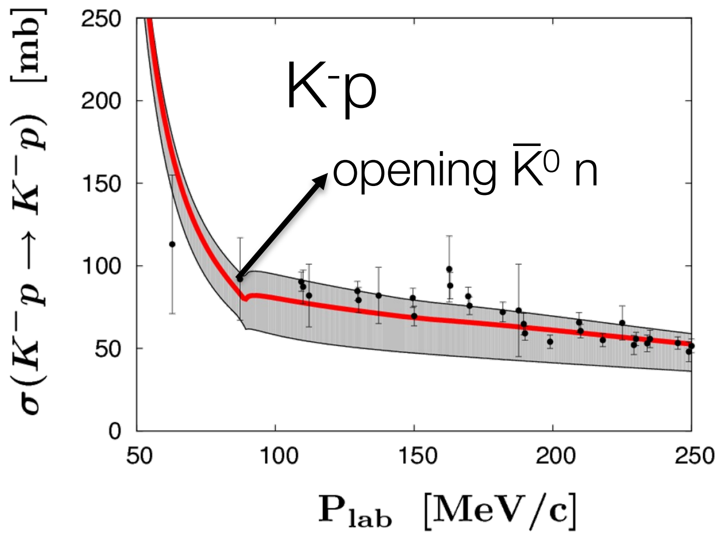

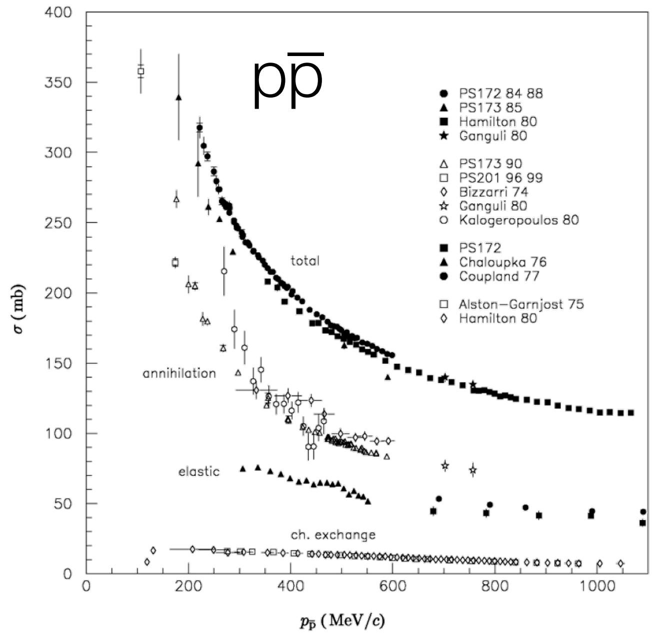

… and now femtoscopy at ALICE

- Fixed final state with the measured pair and all possibe initial states
  - inclusive measurement: 1,2,3,4,… → 1

$$C(k^*) = \zeta(k^*) \cdot \frac{N_{same}(k^*)}{N_{mixed}(k^*)} \begin{cases} > 1 \text{ attraction} \\ = 1 \text{ no inter.} \\ < 1 \text{ repulsion} \end{cases}$$

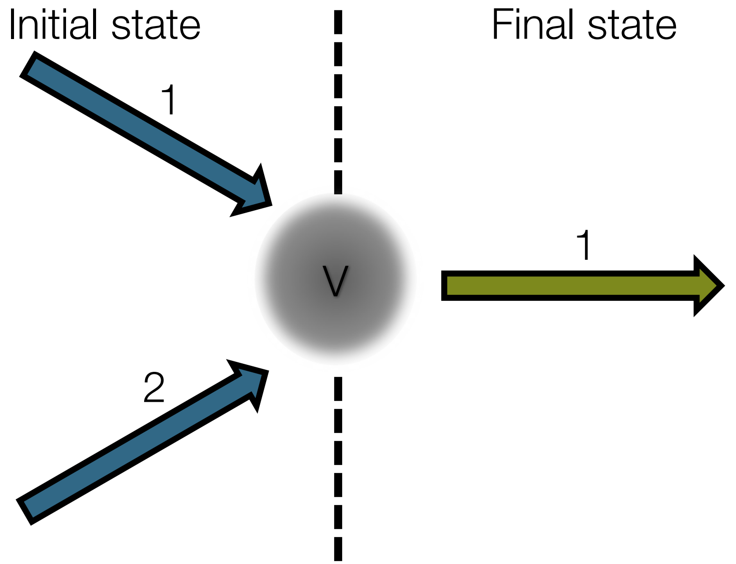

- Access to any particle-pair interaction as long as enough statistics is available
  - Baryon-baryon sector widely investigated in ALICE Run 2

PRC 99 (2019) 024001
PLB 797 (2019) 134822
PRL 123 (2019) 112002
PRL 124 (2020) 09230
PLB 805 (2020) 135419
PLB 811 (2020) 135849
Nature 588 (2020) 232-238
arXiv:2104.04427
arXiv:2105.05578
arXiv:2105.05683
arXiv:2105.05190

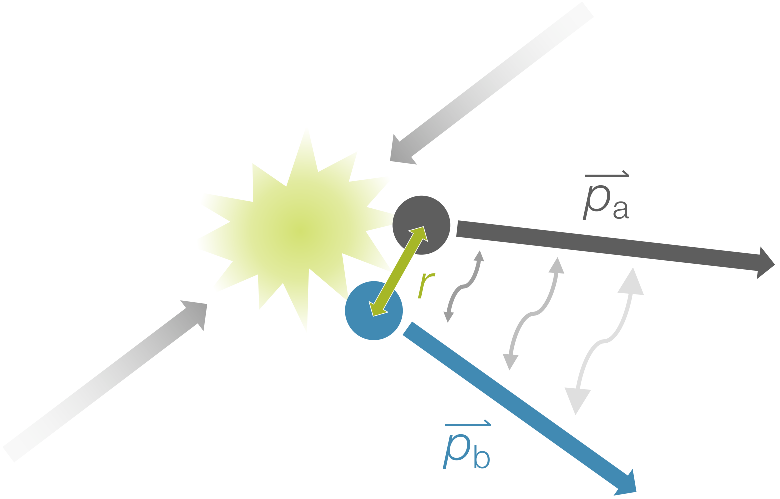

Small Sources: Collective Effects and Strong Resonances

Fit with a 'core' Gaussian + Resonances

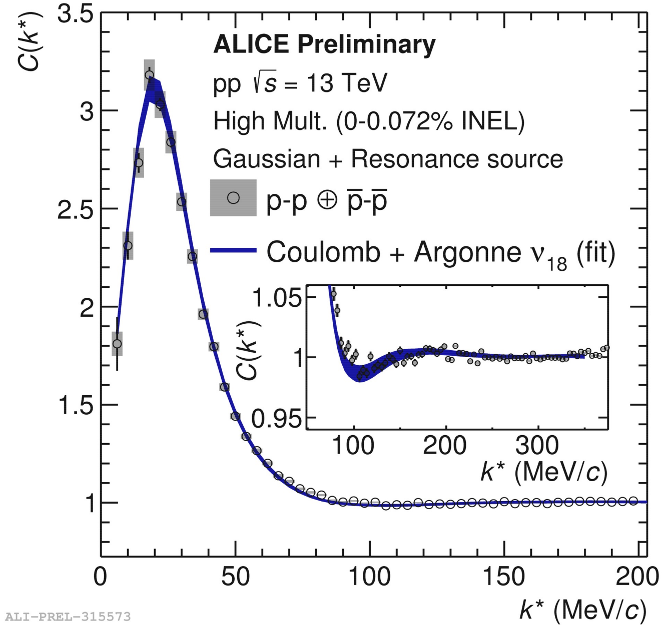

Core Radius

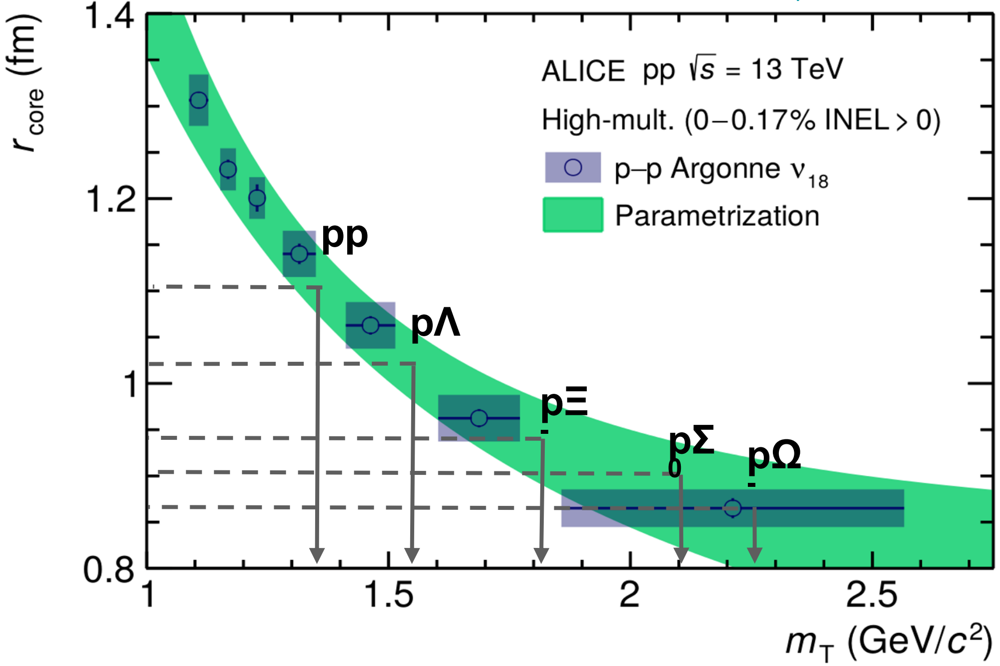

Effective Radius

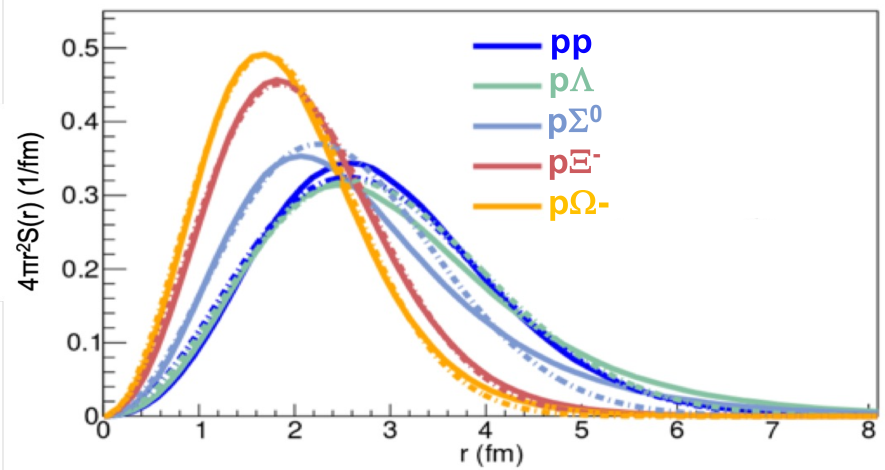

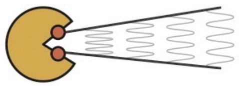

Pair	r_{Core} [fm]	r_{Eff} [fm]
pp	0.96	1.28
pΛ	0.88	1.3
$p\Sigma^0$	0.75	1.12
$p\Xi^-$	0.8	0.92
pΩ-	0.73	0.85

Inelastic channels and source size dependence

- By changing the colliding system we can probe distances ranging from 1 fm up to 10 fm
- become negligible as the source size increases → mostly driven by the elastic interaction

$$C(k^*) = \int S(r)\ |\psi_{1\to1}(k^*,r)|^2\, d^3r + \sum_{j\neq1} w_j \int S(r) \left|\psi_{j\to1}\left(k_j^*, r\right)\right| d^3r$$

$$C(k^*) = \int S(r)\ |\psi_{1\to1}(k^*,r)|^2\, d^3r + \sum_{j\neq1} w_j \int S(r) \left|\psi_{j\to1}\left(k_j^*, r\right)\right| d^3r$$

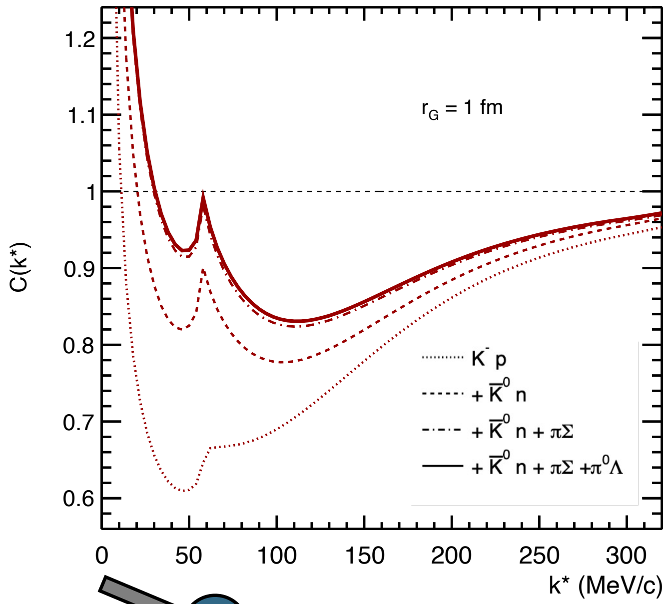

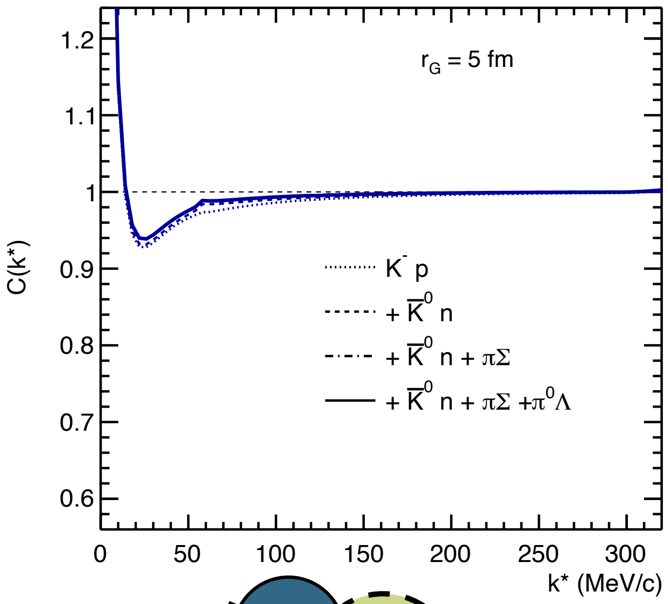

K$^-$–p femtoscopy in ALICE

- First experimental evidence of the opening of $\overline{K}^0$–n channel
- Disappearance of $\overline{K}^0$–n cusp at k*~ 60 MeV/*c* as the source increases
- Pb–Pb data well described by single channel Lednicky-Lyuboshits formula
  → negligible contribution from inelastic channels

χEFT Kyoto model:
Ikeda et al. NPA 881 (2012), PLB706 (2011)
Kamiya et al. PRL 124 (2020)
Mihayara et al. PRC95 (2017)
CATS:
D. Mihaylov, VMS et al. EPJC 78 (2019)

ALICE Coll. Phys.Rev.Lett. 124 (2020)

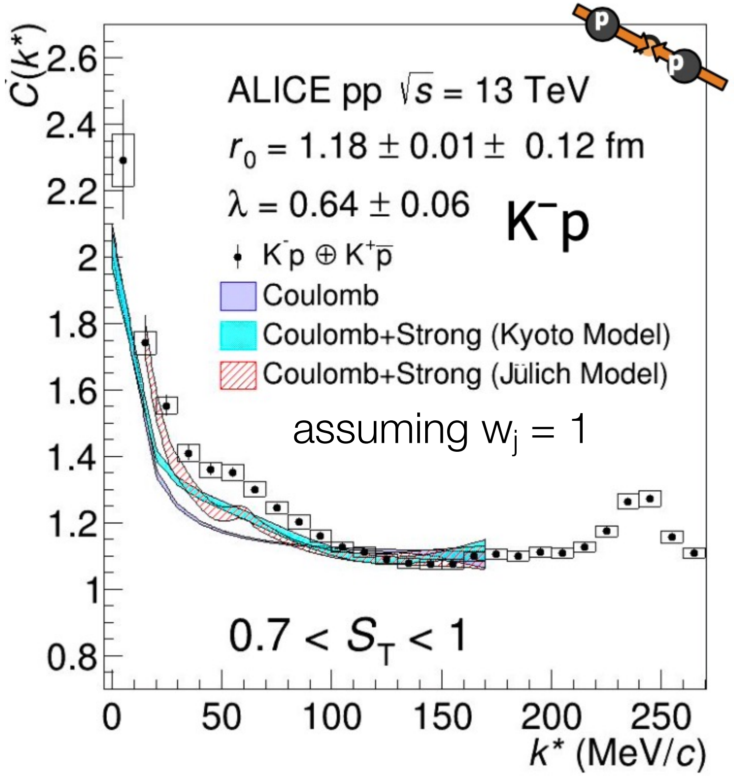

ALICE Coll. Phys.Lett.B 822 (2021)

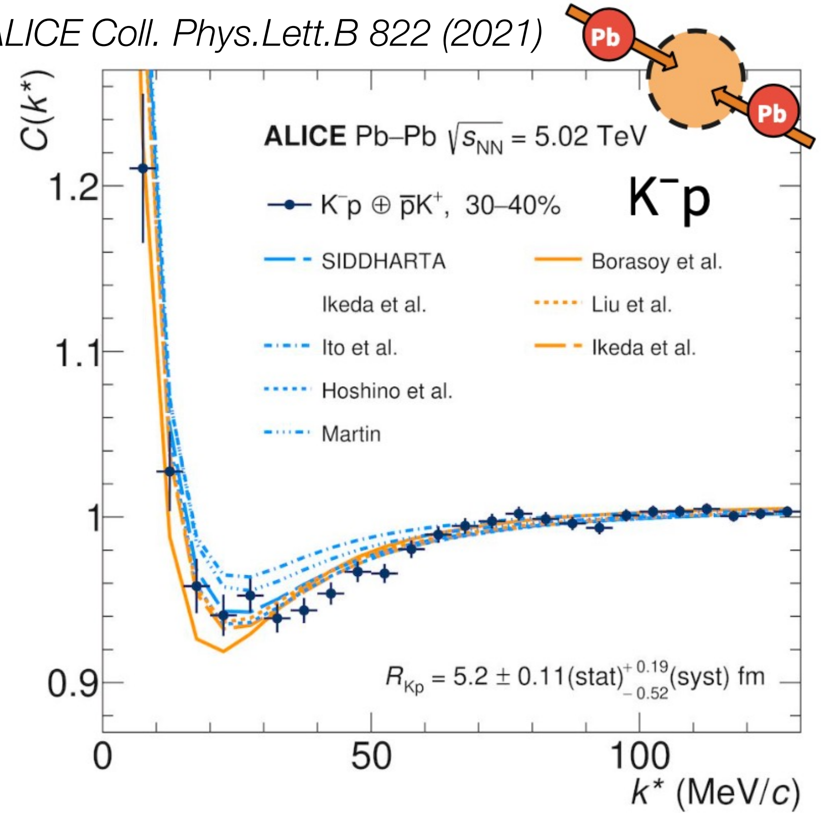

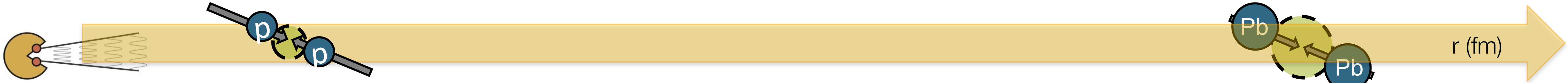

Chiral potentials for K-p updated

- Modification of the conversion weights leads to a better agreement with the data
  - *see Phys.Rev.Lett. 124 (2020) 13, 132501*

Y. Kamiya et al. Phys.Rev.Lett. 124 (2020) 13, 132501

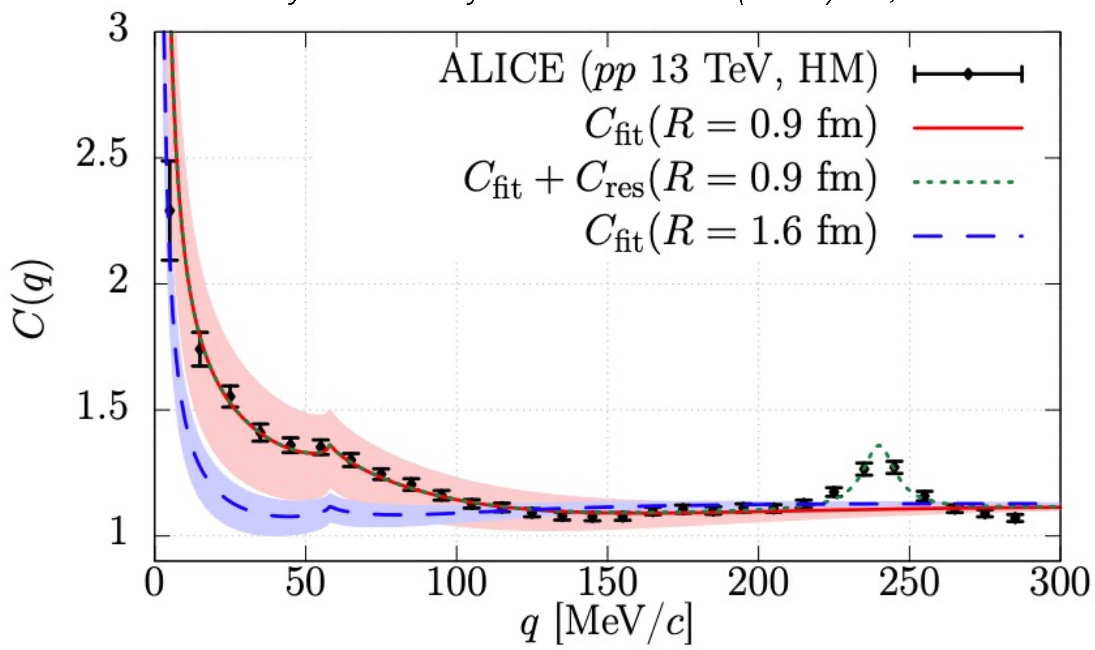

K⁺p emitting source in small colliding systems

- Coulomb + strong chiral potential (K. Aoki and D. Jido, PTEP (2019) 013D01, K. Miyahara, et al, PRC 98 (2018))

$$C(k^*) = \int S(\vec{r}^{\,*}) \left|\psi_{\mathrm{K^+p}}(\vec{k}^*, \vec{r}^{\,*})\right|^2 d^3\vec{r}^{\,*}$$

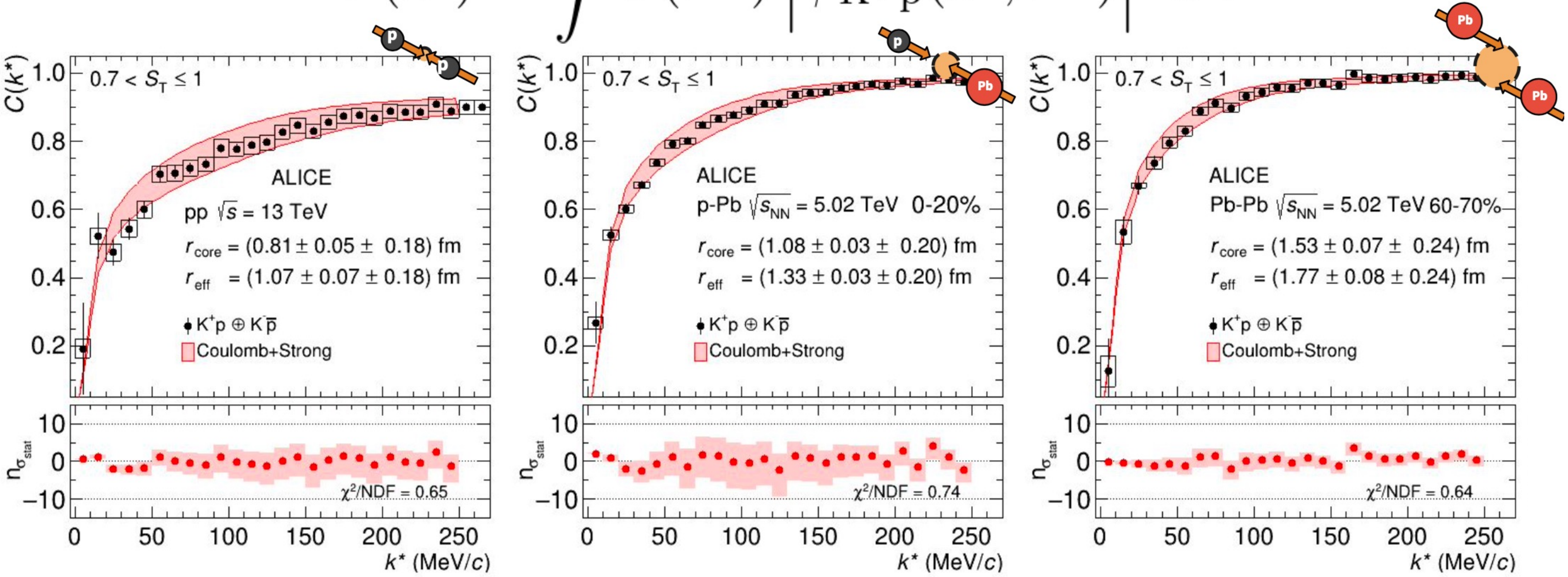

ALICE Coll. Phys.Rev.Lett. 124 (2020) 9, 092301
ALICE Coll. arXiv:2205.15176, accepted by EPJC

K⁺p correlations for large source sizes

- Source size determination anchored to K⁺p
  - assumed Gaussian source
  - Lednicky-Lyuboshits formula to extract r_{eff}

- Large system: no coupled channels effects
- Lednický-Lyuboshitz formula (LL) fit to extract scattering parameters (agreement with Siddharta experiment)

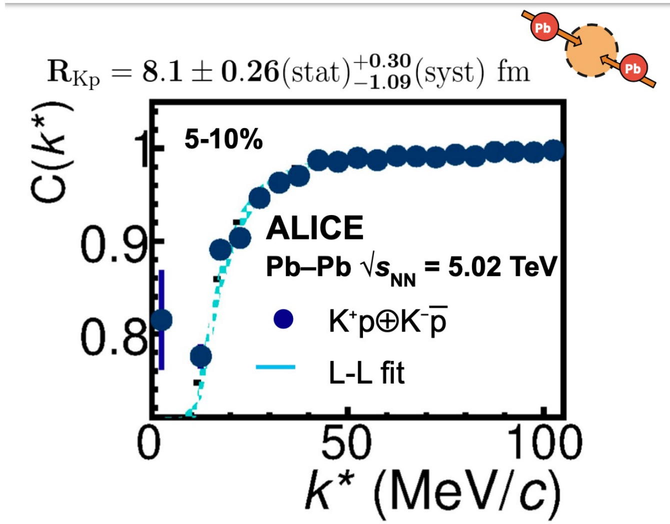

ALICE Coll. PLB 822 (2021)

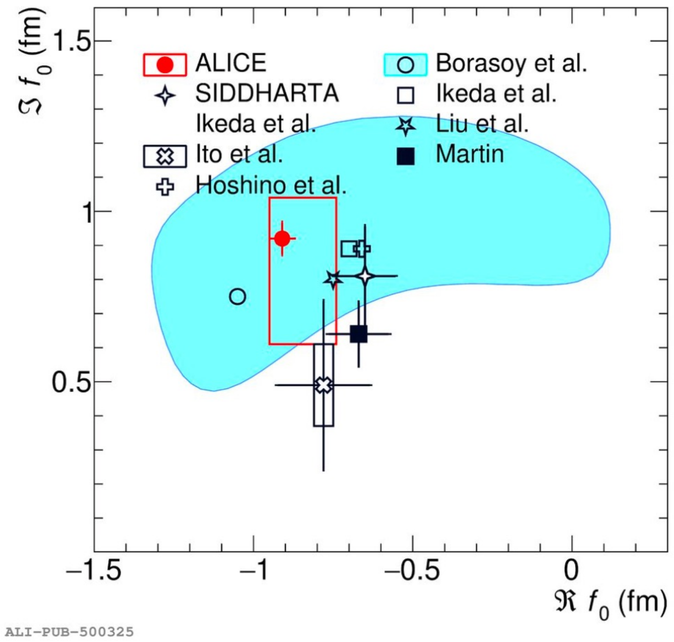

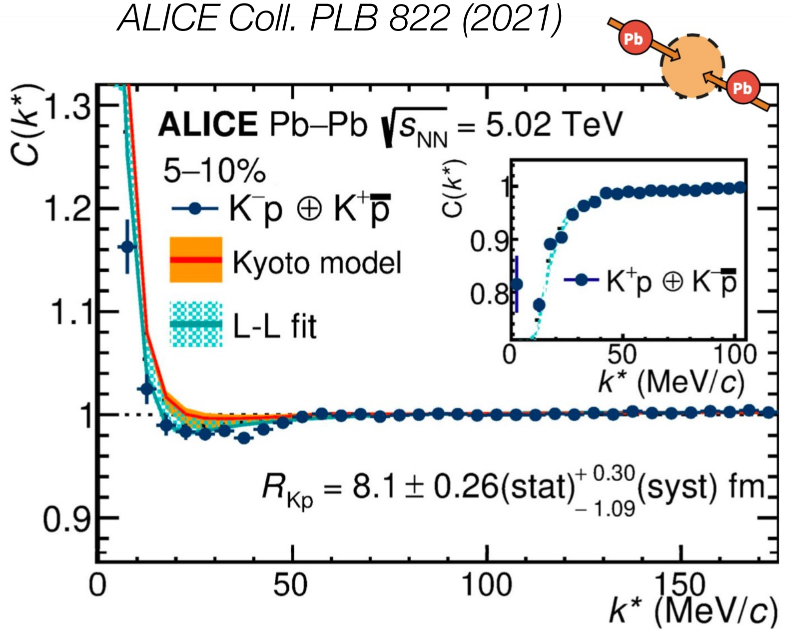

Kp p-Pb results

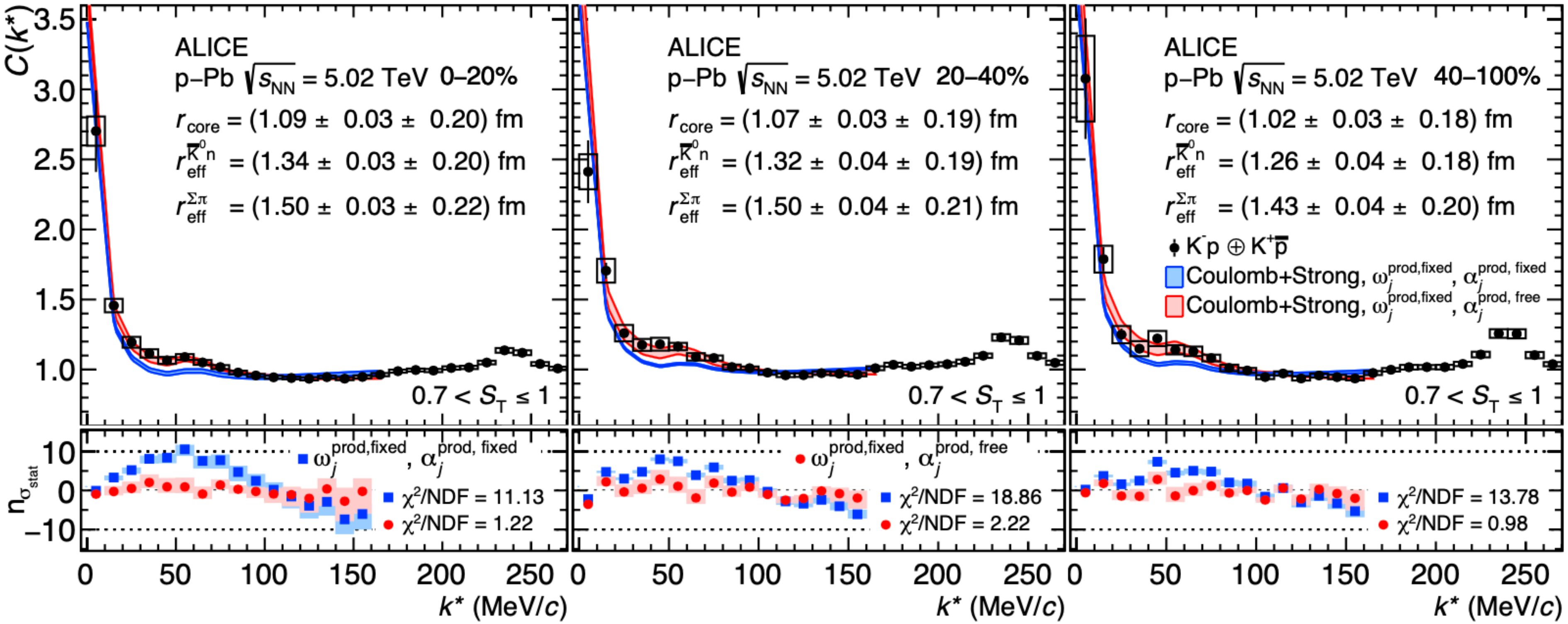

Kp Pb-Pb results

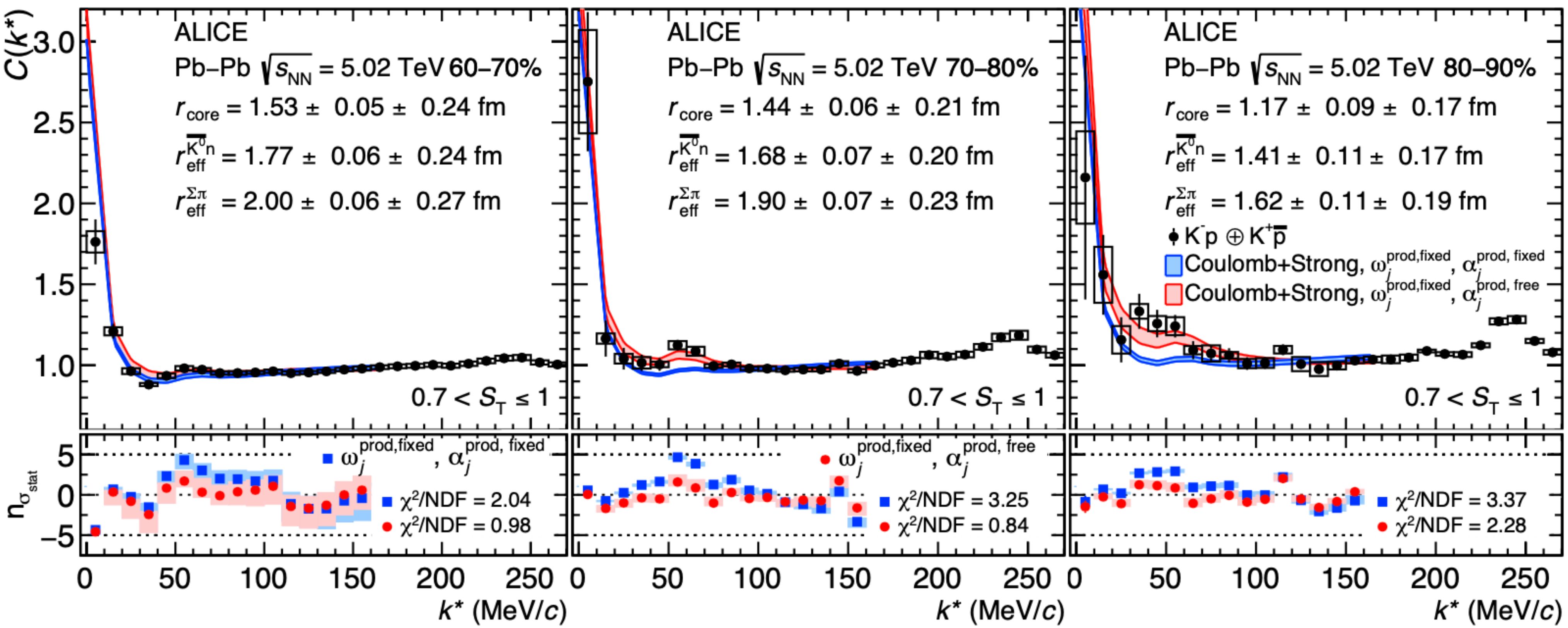

Conversion weights and thermal production

- Thermal Fist parameters anchored to each of the data samples analysed (avg. mult.)
- Only primary particles considered
  - feed from strongly decaying resonances included in the modeling of the source

System	$\mathcal{M}$	T_{ch} (MeV)	γ_s	dV/dy (fm^3)
pp, $\sqrt{s}$ =13 TeV	$6.94^{+0.10}_{-0.08}$	171±1	0.78±0.06	16.66±1.39
p–Pb, 0–20%	35.42±1.44	167±1	0.86±0.33	85.01±7.08
p–Pb, 20–40%	23.12±0.52	168±1	0.83±0.20	55.49±4.62
p–Pb, 40–100%	9.88±0.42	170±1	0.79±0.09	23.71±1.98
Pb–Pb, 60–70%	96.3±5.8	164±1	0.95±0.59	231.12±19.26
Pb–Pb, 70–80%	44.9±3.4	166±1	0.88±0.43	107.76±8.98
Pb–Pb, 80–90%	17.52±1.89	169±1	0.81±0.15	42.05±3.50

Pairs	pp	p–Pb			Pb–Pb		
	$\sqrt{s}$ = 13 TeV, MB	0–20%	20–40%	40–100%	60–70%	70–80%	80–90%
	$\mathcal{M} = 6.94^{+0.10}_{-0.08}$	$\mathcal{M}$ = 35.42 ± 1.44	$\mathcal{M}$ = 23.12±0.52	$\mathcal{M}$ = 9.88±0.42	$\mathcal{M}$ = 96.3±5.8	$\mathcal{M}$ = 44.9±3.4	$\mathcal{M}$ = 17.52±1.89
K^-p	1.00	1.00	1.00	1.00	1.00	1.00	1.00
$\overline{K}^0 n$	0.97 ± 0.20	0.98 ± 0.20	0.97 ± 0.20	0.99 ± 0.20	0.99 ± 0.20	0.99 ± 0.20	0.99 ± 0.20
$\pi^-\Sigma^+$	1.41 ± 0.70	1.41 ± 0.70	1.35 ± 0.67	1.27 ± 0.63	1.46 ± 0.73	1.38 ± 0.69	1.30 ± 0.65
$\pi^+\Sigma^-$	1.42 ± 0.71	1.42 ± 0.71	1.35 ± 0.67	1.29 ± 0.64	1.47 ± 0.73	1.39 ± 0.69	1.31 ± 0.65
$\pi^0\Sigma^0$	1.37 ± 0.68	1.41 ± 0.70	1.38 ± 0.70	1.22 ± 0.61	1.46 ± 0.73	1.38 ± 0.69	1.31 ± 0.65
$\pi^0\Lambda$	1.96 ± 0.93	2.07 ± 1.03	1.96 ± 0.93	1.86 ± 0.93	1.48 ± 0.74	1.40 ± 0.70	1.32 ± 0.66

V. Vovchenko et al., PRC 100 no. 5 (2019))
E. Schnedermann et al., PRC 48 (1993)
ALICE Coll., PLB 728 (2014)
ALICE Coll., PRC 101 no. 4 (2020)

Results on Λ-$\bar{\Lambda}$ and p-$\bar{\Lambda}$ femtoscopy

- Estimates based on kinematics (EPOS) and SU(3) flavour symmetry for 2-meson channels (ππ,πK)
  - similar amount of p-$\bar{\Lambda}$ and Λ-$\bar{\Lambda}$ pairs at low k* (~6.4%)
  - coupling strength from meson-baryon SU(3) lagrangian for p-$\bar{\Lambda}$ ~ 3 times larger than Λ-$\bar{\Lambda}$

$$\frac{g_{2M\to p-\bar{\Lambda}} \times N_{2M\to p-\bar{\Lambda}}}{g_{2M\to \Lambda-\bar{\Lambda}} \times N_{2M\to \Lambda-\bar{\Lambda}}} \approx 6.3$$

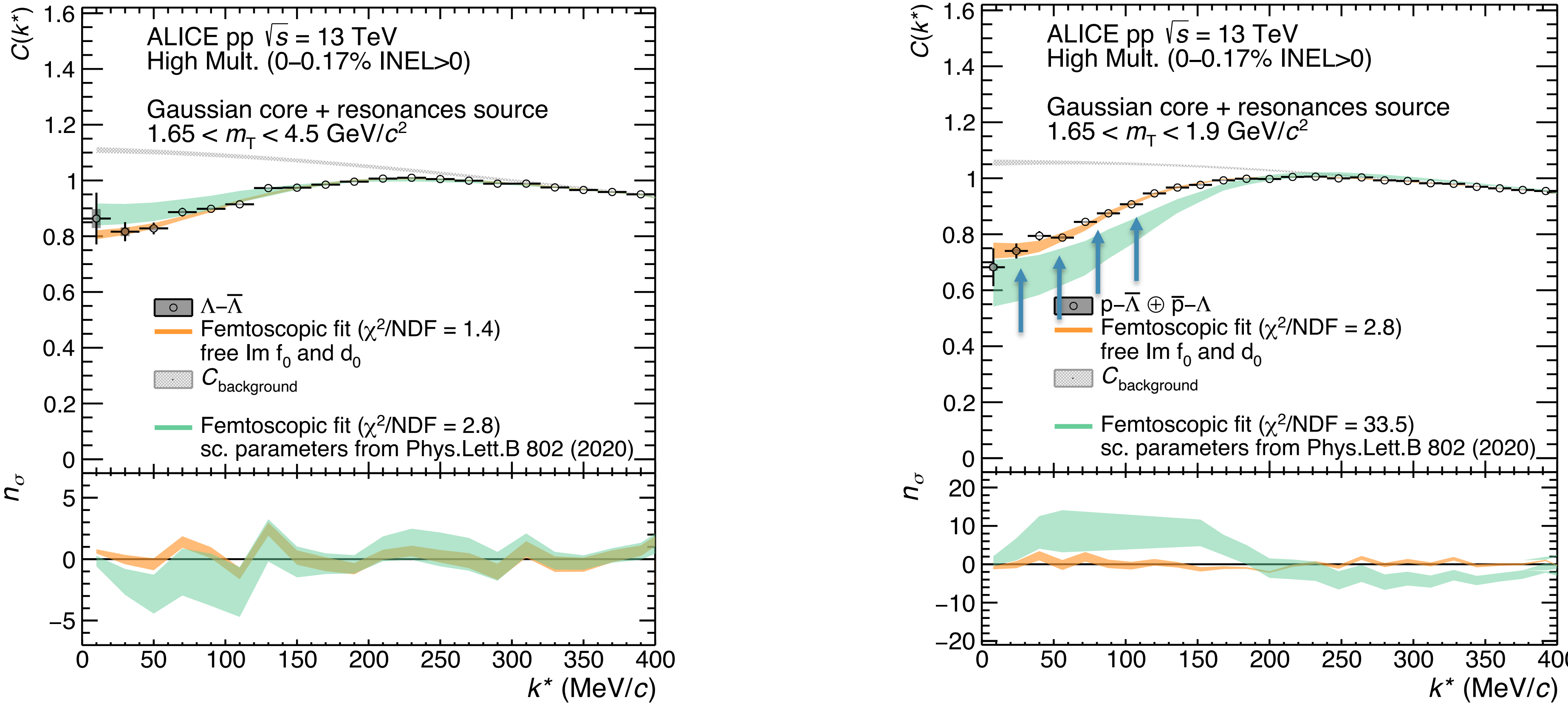

ALICE Coll. PLB 829 (2022)

Conversion weights in Kp femtoscopy

$$C(k^*) = \int S(r)\, \left|\psi_{1\to 1}(k^*, r)\right|^2 d^3r + \sum_{j=\Sigma\pi,\bar{K}^0 n} w_j^{prod} \int S_j(r)\, \left|\psi_{j\to 1}(k_j^*, r)\right|^2 d^3r$$

- Each coupled-channel is taken into account in ω_j weights
  - primary production yields fixed from thermal model (Thermal-FIST V. Vovchenko et al., PRC 100 no. 5 (2019))
  - estimate amount of pairs in kinematic region sensitive to final state interactions
  - distribute particles according to blast-wave model(*)
  - normalize to expected yield of K–p

(*) E. Schnedermann et al., PRC 48 (1993)
ALICE Coll., PLB 728 (2014)
ALICE Coll., PRC 101 no. 4 (2020)

Results on p-$\bar{\text{p}}$: modeling the correlation

elastic

n-$\bar{\text{n}}$ → p-$\bar{\text{p}}$

$$C_{\text{p}-\bar{\text{p}}}(k^*) = \int S(r)|\psi_{p\bar{p}\to p\bar{p}}|^2 d^3r + \int S(r)|\psi_{n\bar{n}\to p\bar{p}}|^2 d^3r$$

- Chiral Effective Field Theory at N^{3}LO (with n-$\bar{\text{n}}$ coupled-channel) wavefunctions with Coulomb
  - S and P waves, tuned to scattering data and protonium

J. Haidenbauer et al. JHEP 1707 (2017)
D.Mihailov et al. Eur.Phys.J.C 78 (2018) 5, 394
Haidenbauer et al.,PRD 92 (2015) 5, 054032

Results on p-p̄: modeling the correlation

elastic — n-n̄ → p-p̄ — multi-meson annihilation channels

$$C_{p-\bar{p}}(k^*) = \int S(r)|\psi_{p\bar{p}\to p\bar{p}}|^2 d^3r + \int S(r)|\psi_{n\bar{n}\to p\bar{p}}|^2 d^3r + \sum_{PW} \rho_{PW}\,\omega_{PW} \int S(r)|\psi^{PW}_{p\bar{p}\to p\bar{p}}|^2 d^3r$$

- Chiral Effective Field Theory at N^{3}LO (with n-n̄ coupled-channel) wavefunctions with Coulomb
  - S and P waves, tuned to scattering data and protonium
- Approximate inclusion of annihilation channels (X→ p-p̄) using the Migdal-Watson approximation
  - elastic WF rescaled by a coupling weight ω_{PW} to be fitted to data
  - Investigation on the shape of each PWs to reduce number of parameters
    - $^1S_0$ for S states
    - $^3P_0$ and $^1P_1$ for P states
- Calculations performed with CATS framework

J. Haidenbauer et al. JHEP 1707 (2017)
D.Mihailov et al. Eur.Phys.J.C 78 (2018) 5, 394
Haidenbauer et al.,PRD 92 (2015) 5, 054032

Results on p-$\bar{p}$: modeling the correlation

- No cusp of n-$\bar{n}$ opening at k*~ 50 MeV/c → in agreement with charge-exchange cross-sections
- rise of CF at low k*
  - no agreement with Coulomb only
  - χEFT calculations with no explicit CC terms do not reproduce the data at low k*
  - evidence of annihilation channels feeding into p-$\bar{p}$ pairs

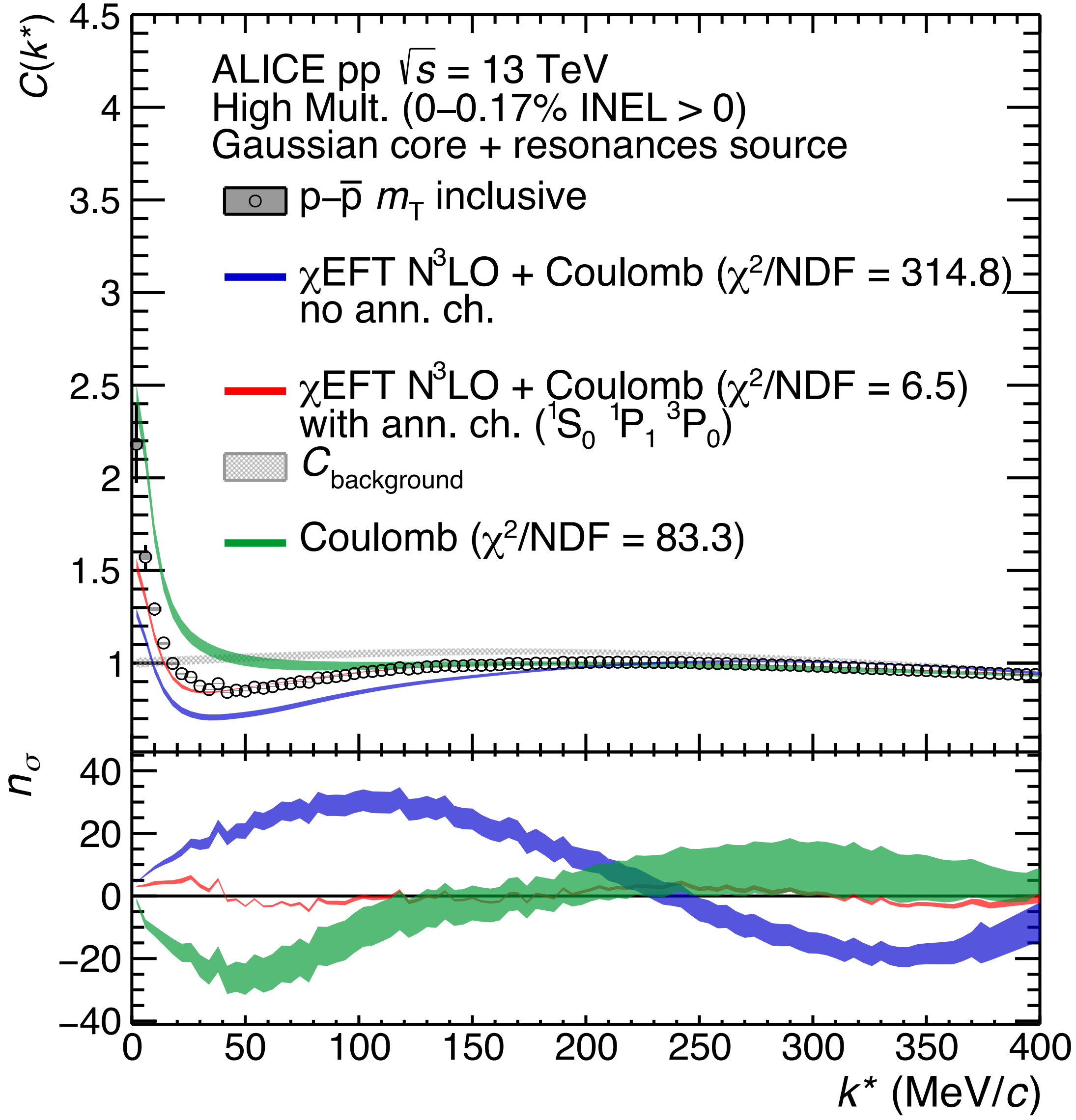

ALICE Coll. arXiv: 2105.05190

Correlation function for p-p̄

- No cusp of n-n̄ opening at k*~ 50 MeV/c → in agreement with charge-exchange cross-sections
- rise of CF at low k*
  - no agreement with Coulomb only
  - χEFT calculations with no explicit CC terms do not reproduce the data at low k*
  - evidence of annihilation channels feeding into p-p̄ pairs
- Annihilation channels **X→ p-p̄ included**
  - better agreement with the data is obtained
  - Dominant coupling weights in $^3P_0$ and $^1S_0$

ω_{3P0}= 40.04 ± 4.06 (stat) ± 4.24 (syst)

ω_{1S0}= 1.19 ± 0.10 (stat) ± 0.19 (syst)

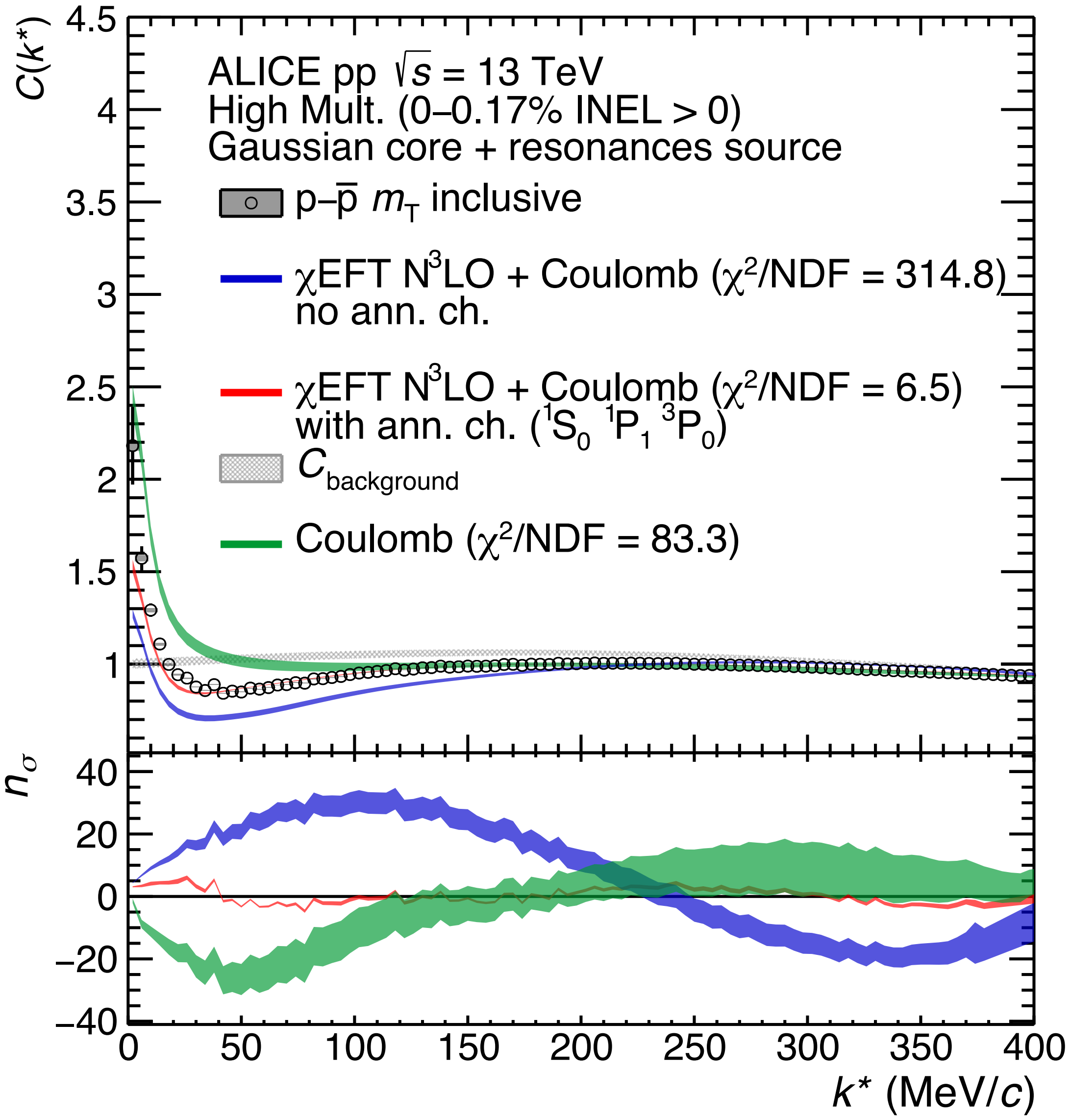

PWA: D.Zhou and R.G. E. Timmermans PRC86 (2012)

ALICE Coll. arXiv: 2105.05190

Comparison Pb–Pb and pp data in B-antiB

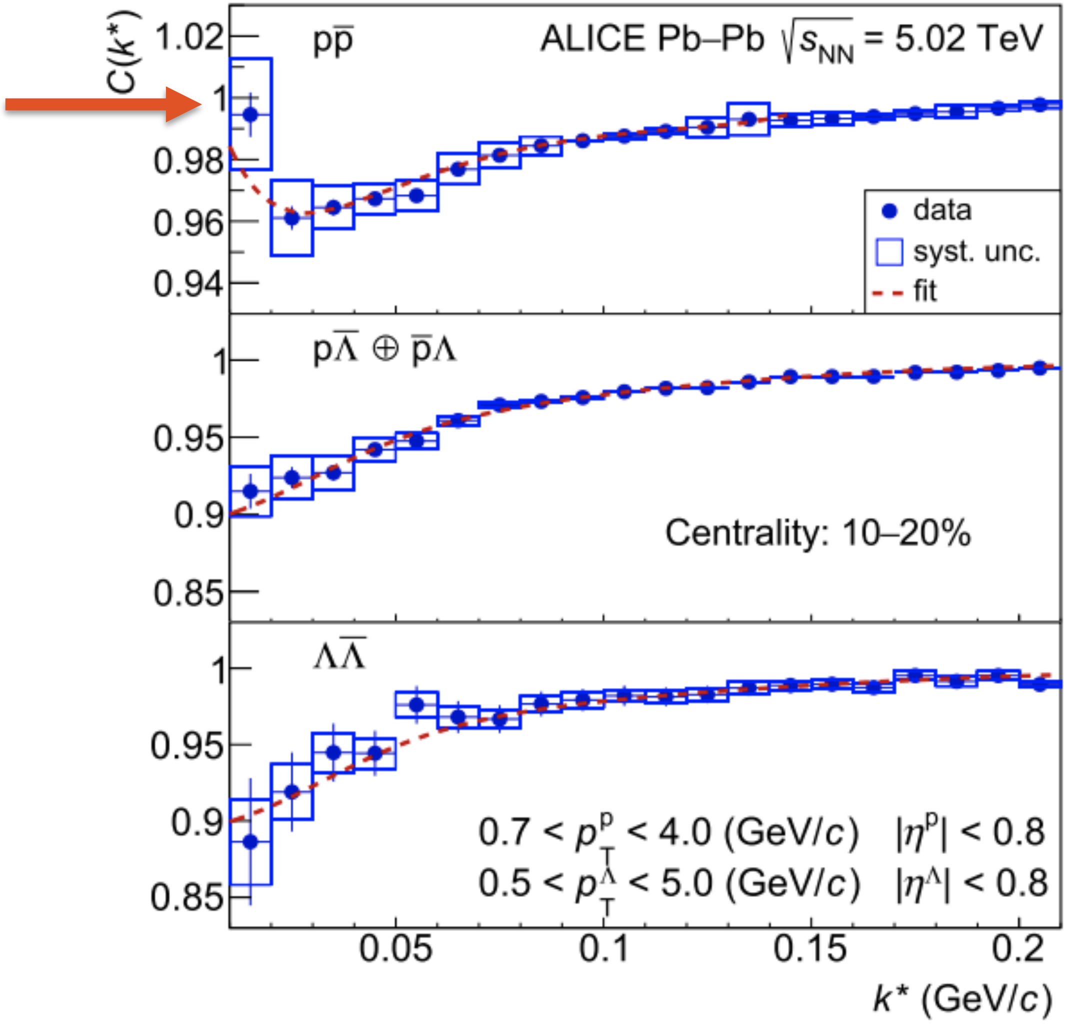

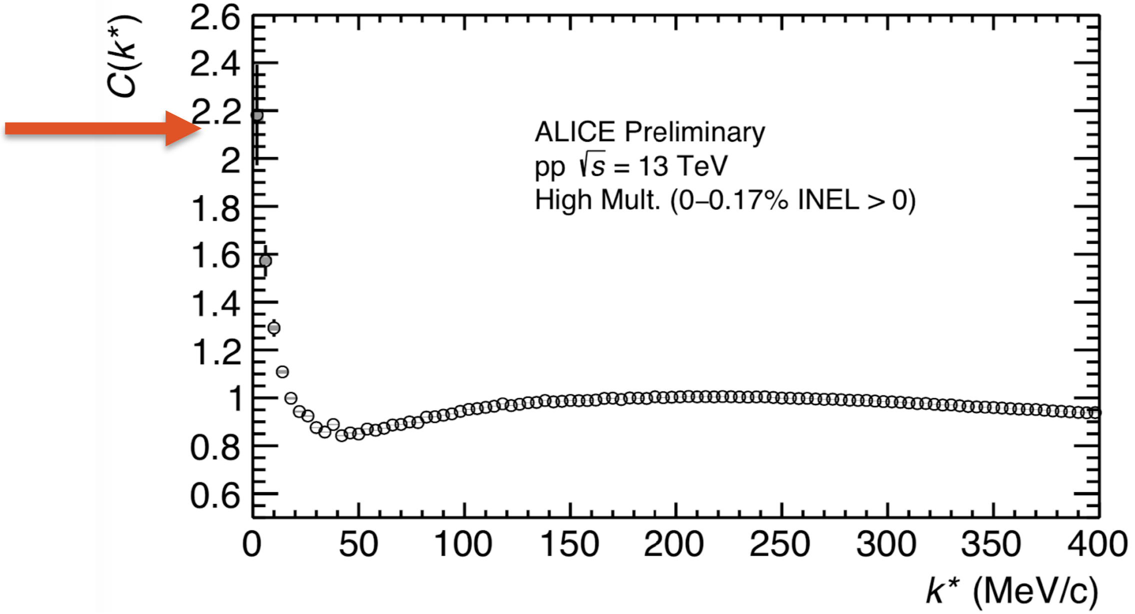

Comparison Pb–Pb and pp data in B-antiB

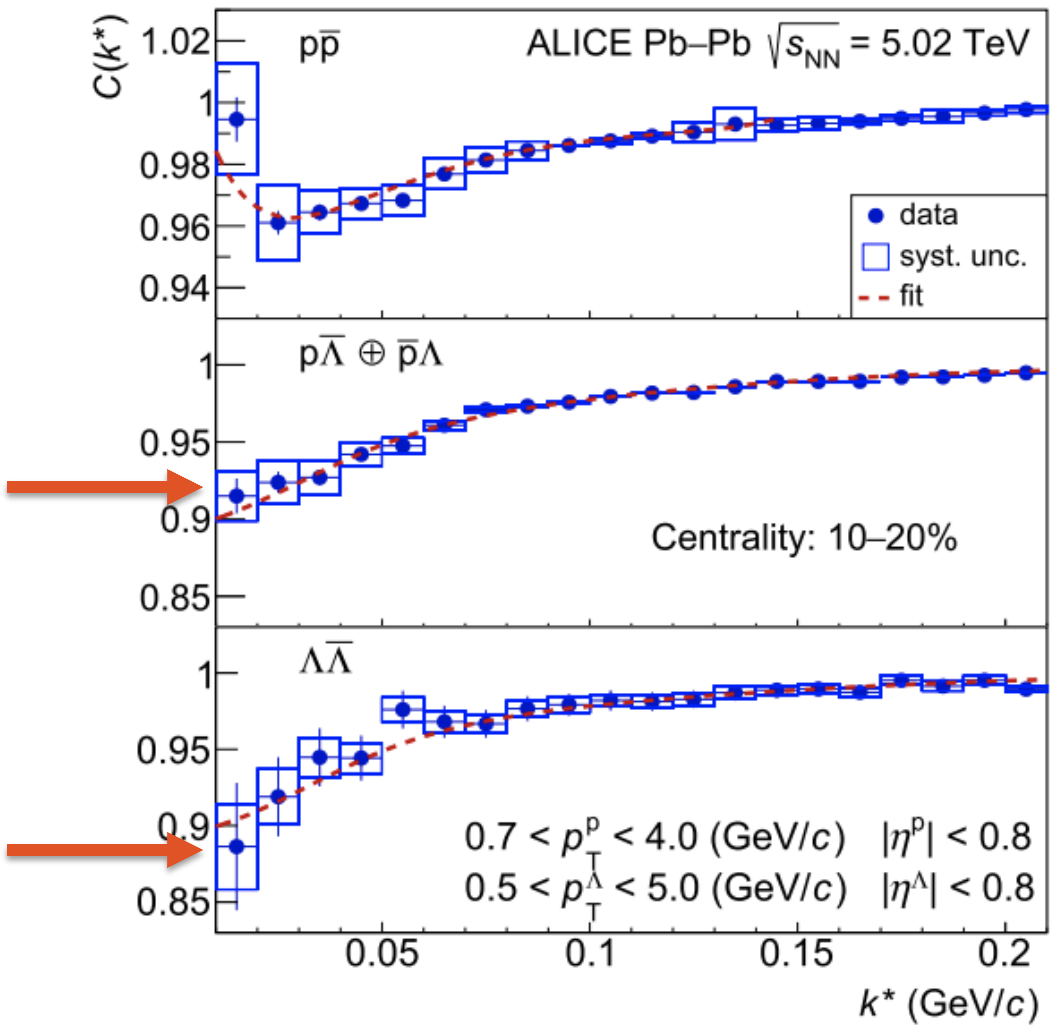

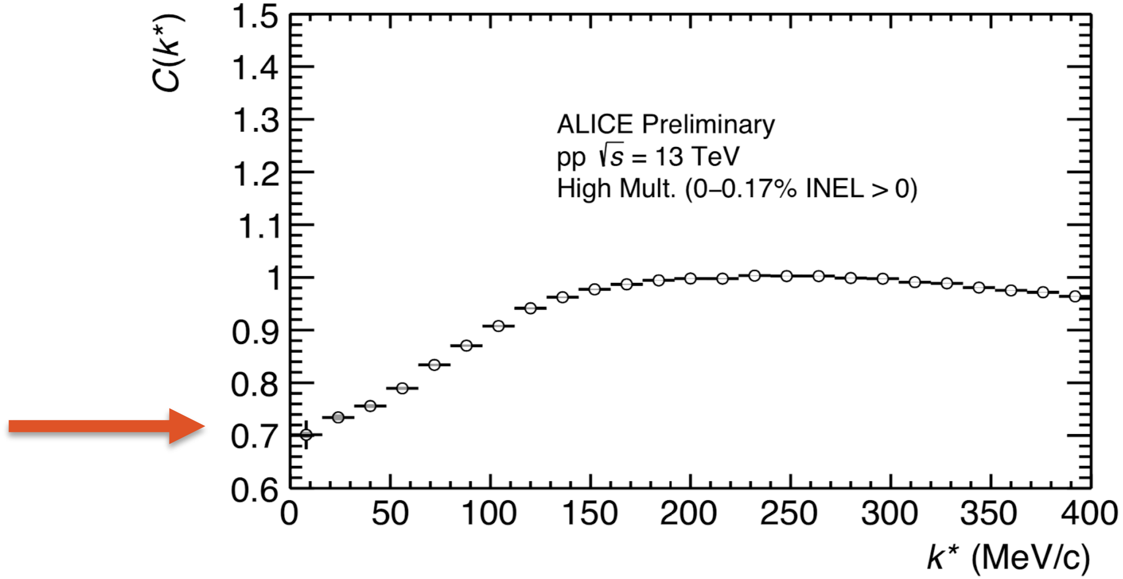

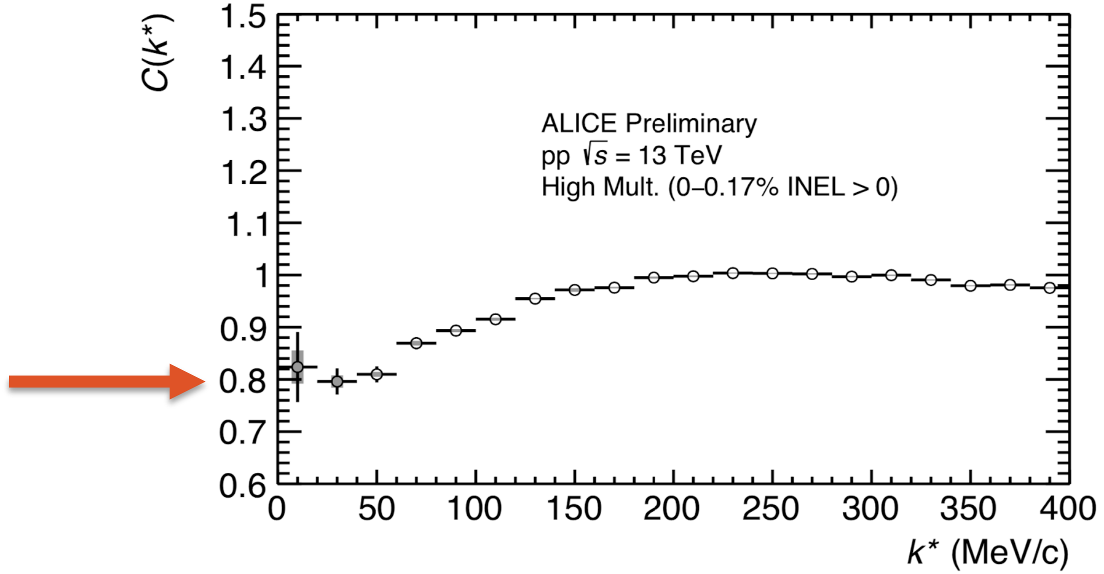

Coupled channel wave functions

- Pairs close in mass with the same quantum numbers: e.g. p–Ξ^- and Λ–Λ
- Schrödinger equation of one pair → Equation system of all 1, … , N pairs

$$\hat{\mathcal{H}} \cdot \psi = \mathrm{E} \cdot \psi \mapsto \begin{pmatrix} \hat{\mathcal{H}}_{11} & \cdots & \hat{\mathcal{H}}_{1\mathrm{N}} \\ \vdots & \ddots & \vdots \\ \hat{\mathcal{H}}_{\mathrm{N}1} & \cdots & \hat{\mathcal{H}}_{NN} \end{pmatrix} \cdot \begin{pmatrix} \psi_1 \\ \vdots \\ \psi_N \end{pmatrix} = E \cdot \begin{pmatrix} \psi_1 \\ \vdots \\ \psi_N \end{pmatrix}$$

-

1) Coupled channels influence the elastic channels of the two-particle wave function ψ_j